Nuclear Structure in Astrophysics – Recent Examples from the S-DALINAC

- S-DALINAC and research program – an overview
- Selected examples:
  - Deuteron electrodisintegration under 180° and its importance for the primordial nucleosynthesis of the lightest nuclei
  - Possible role of ^{9}Be in the production of ^{12}C
  - Electron scattering on ^{12}C and the structure of the Hoyle state
  - Electron scattering on *fp*-shell nuclei and supernova inelastic neutrino-nucleus cross sections
  - Neutrino nucleosynthesis of the exotic odd-odd nuclei ^{138}La and ^{180}Ta

Supported by the SFB 634 of the Deutsche Forschungsgemeinschaft

Experiments at the S-DALINAC

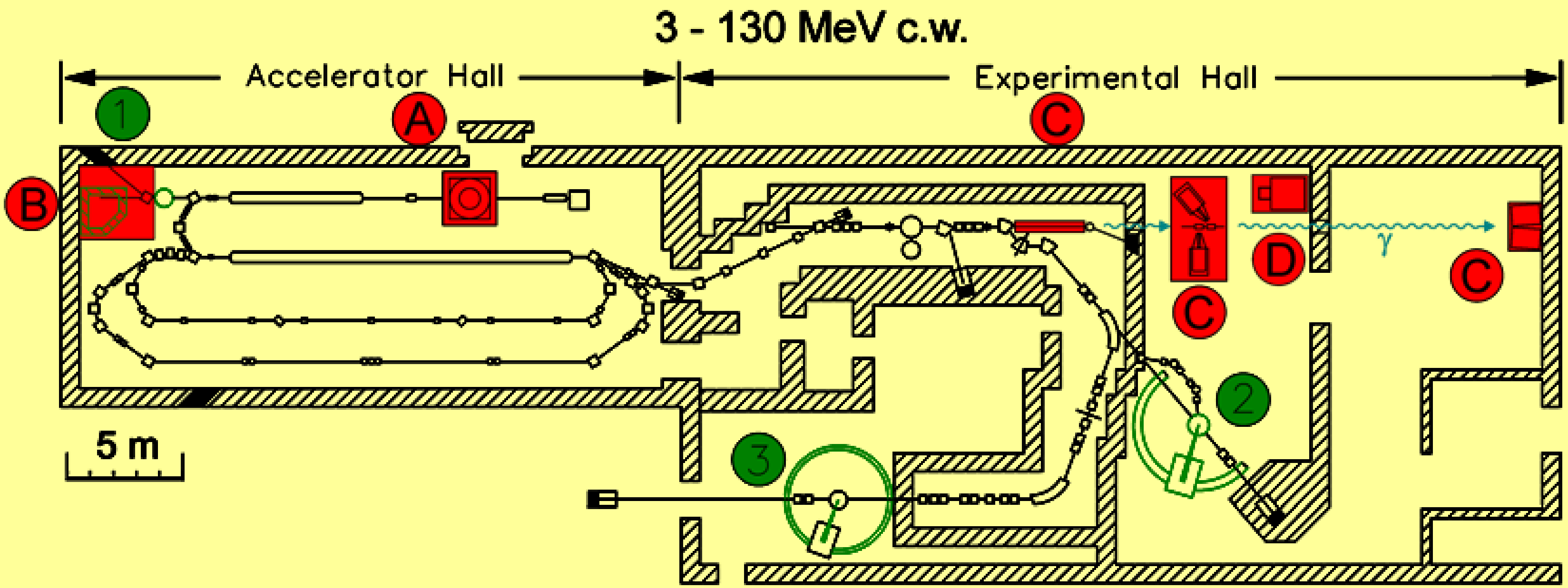

Status

1. Nuclear resonance fluorescence
2. (e,e´) and 180° experiments
3. High-resolution (e,e´) experiments

SFB

- A Polarized electron source
- B 14 MeV bremsstrahlung
- C 100 MeV bremsstrahlung for polarizability of the nucleon
- D Photon tagger

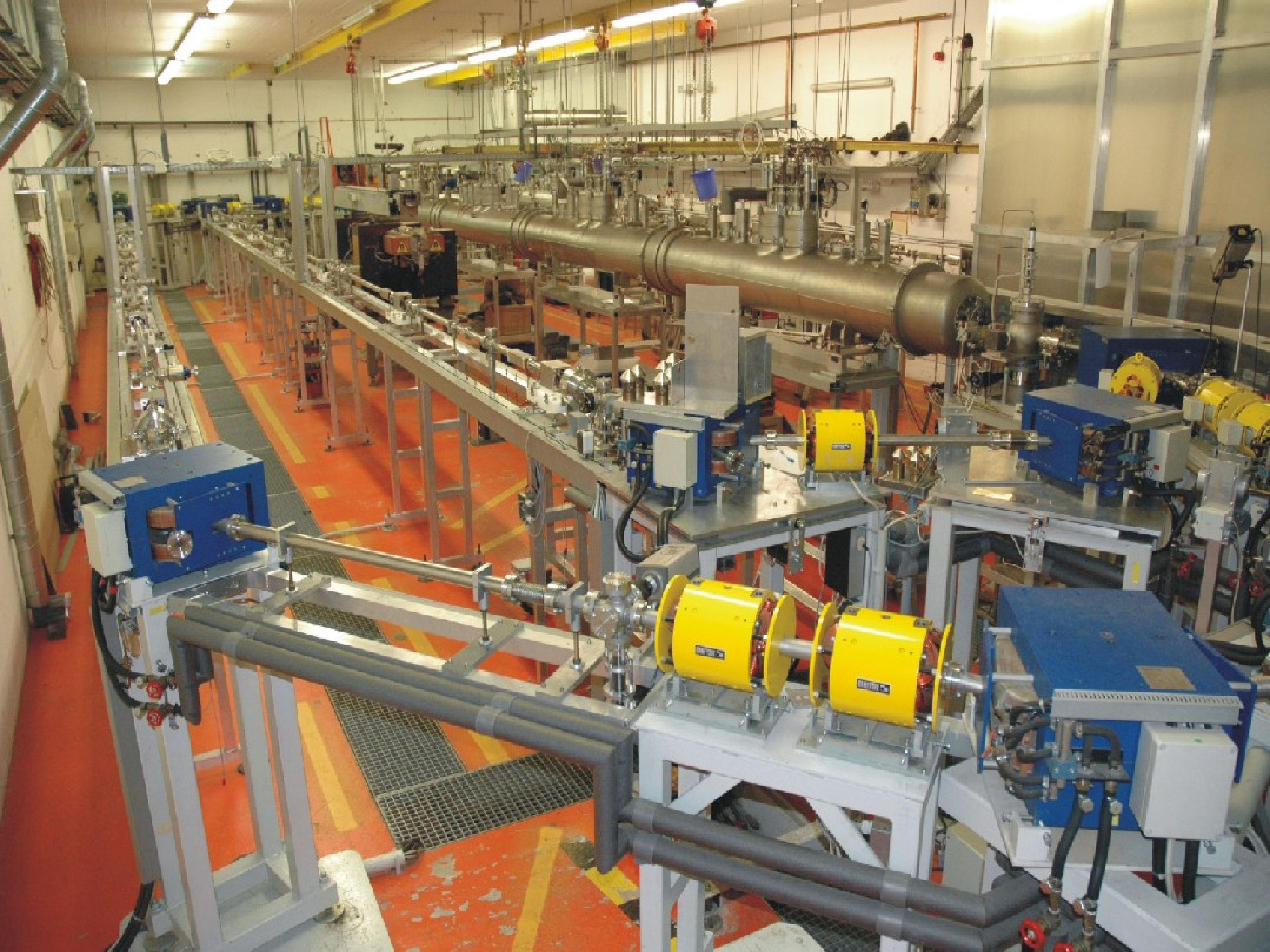

Deuteron electrodisintegration under 180°

- Astrophysical motivation: Big-Bang nucleosynthesis
- Experiment: 180° electron scattering
  - High selectivity
  - High energy resolution
- Precision test of theoretical models
  - NN potentials
  - EFT
- Summary and outlook

N. Ryezayeva *et al.*, to be published

Primordial nucleosynthesis

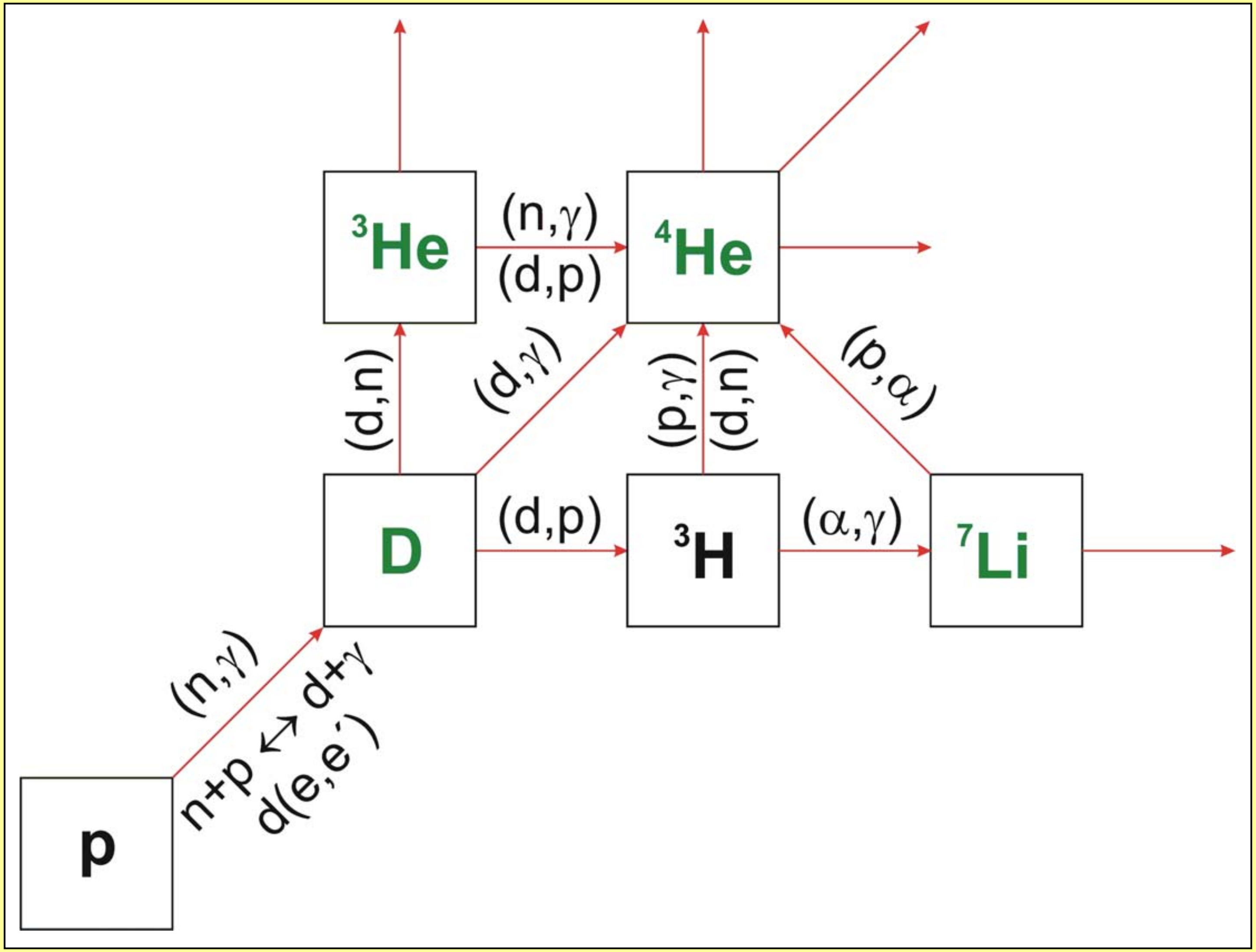

- D, ^{3}He, ^{4}He, ^{7}Li are synthesized

Test of cosmological standard model

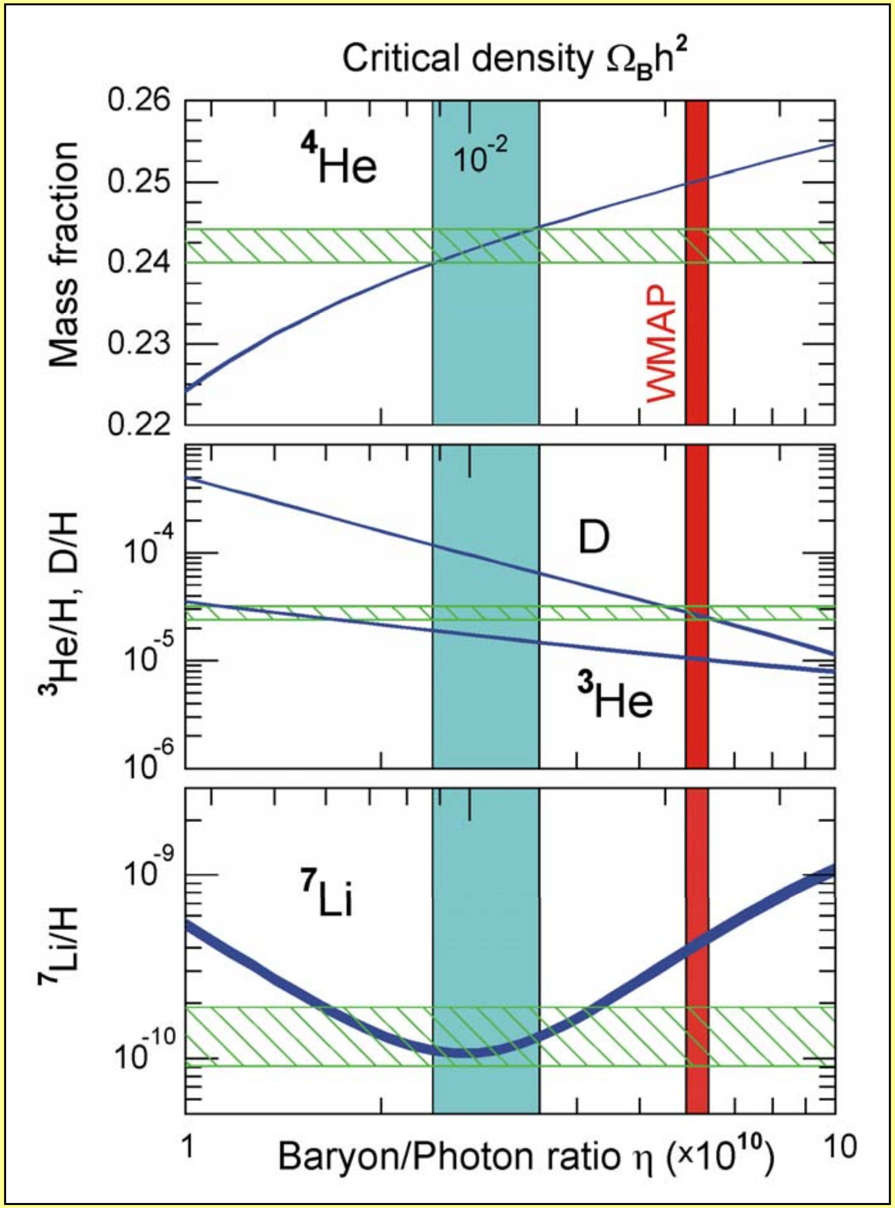

Adopted from A. Coc *et al.*, Ap. J. 600, 544 (2004)

- Abundances depend on baryon/photon ratio (baryon density)
- Observational constraints: WMAP disagrees with spectroscopic information and/or BBN
- Critical density derived from ^{4}He and ^{7}Li is different from D

Uncertainty of ^{7}Li abundance

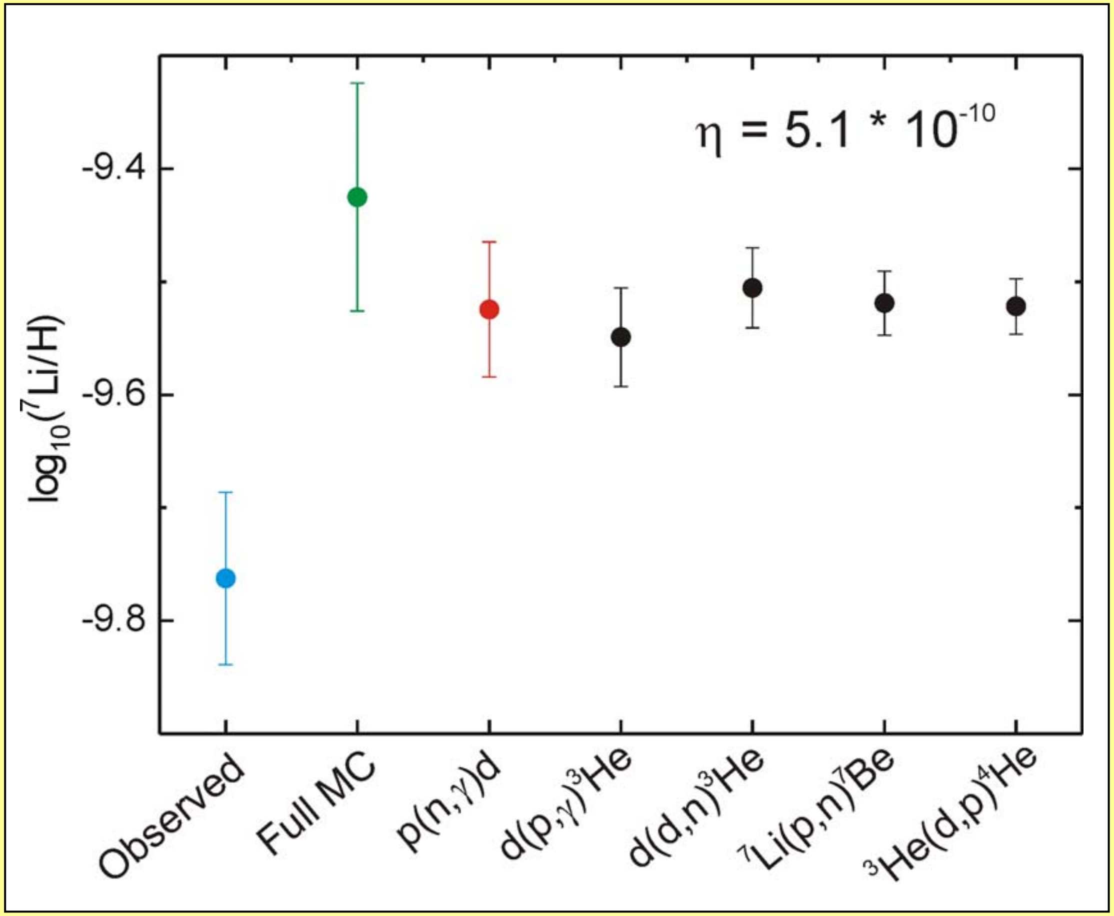

- Largest uncertainty from *p(n,γ)d* reaction
- Relevant energy window 15 - 200 keV above threshold

S. Burles *et al.*, PRL 82, 4176 (1999)

d(γ,*n*)*p*: data and predictions

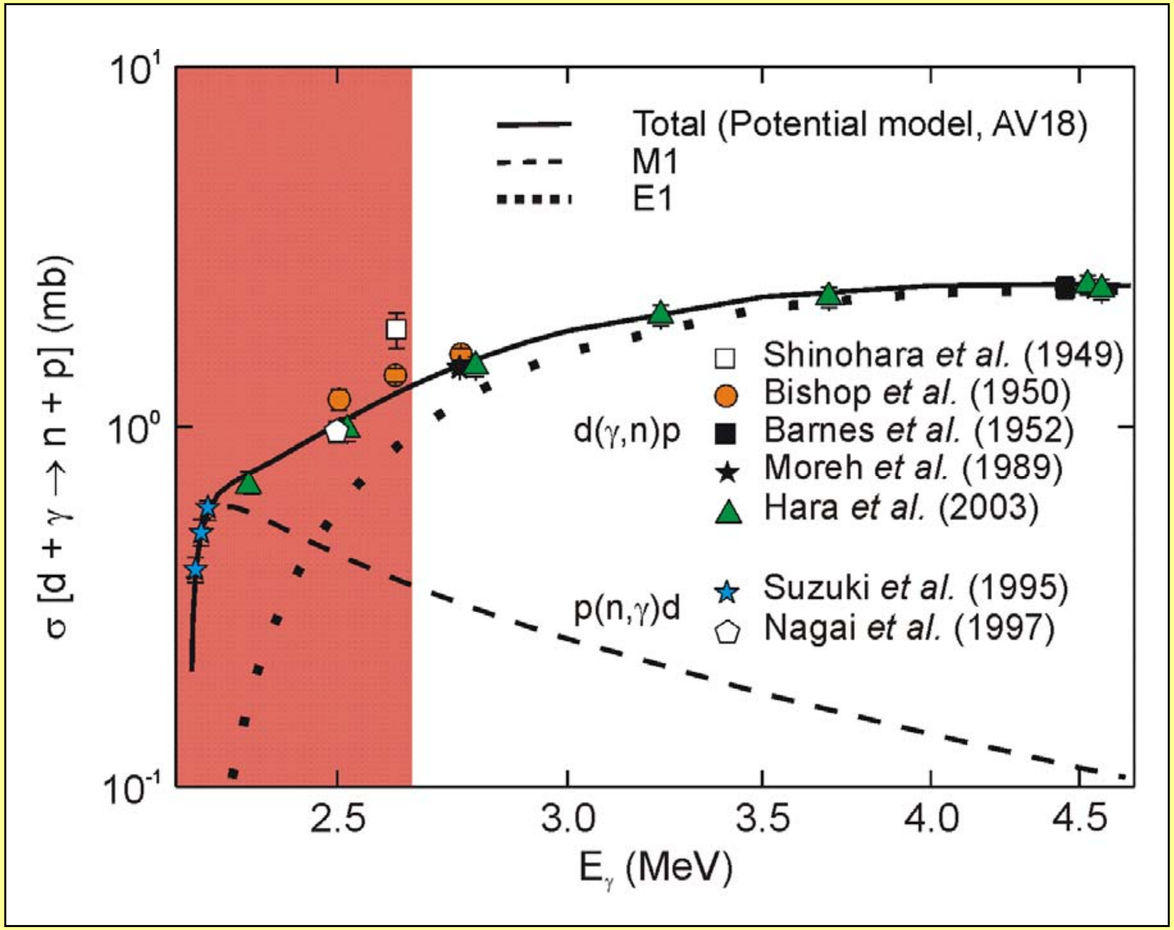

- Potential model (AV18) calculations by H. Arenhövel
- EFT calculations (J.-W. Chen and M.J. Savage, S. Ando *et al.*) are very similar
- Scarce data at the threshold
- *M*1 dominates: *d*(e,e´) at 180°

Why electron scattering under 180°?

$$\left(\frac{d\sigma}{d\Omega}\right) = \left(\frac{d\sigma}{d\Omega}\right)_L + \left(\frac{d\sigma}{d\Omega}\right)_T$$

$$V_L \times \left|F_L(q)\right|^2 \qquad V_T \times \left|F_T(q)\right|^2$$

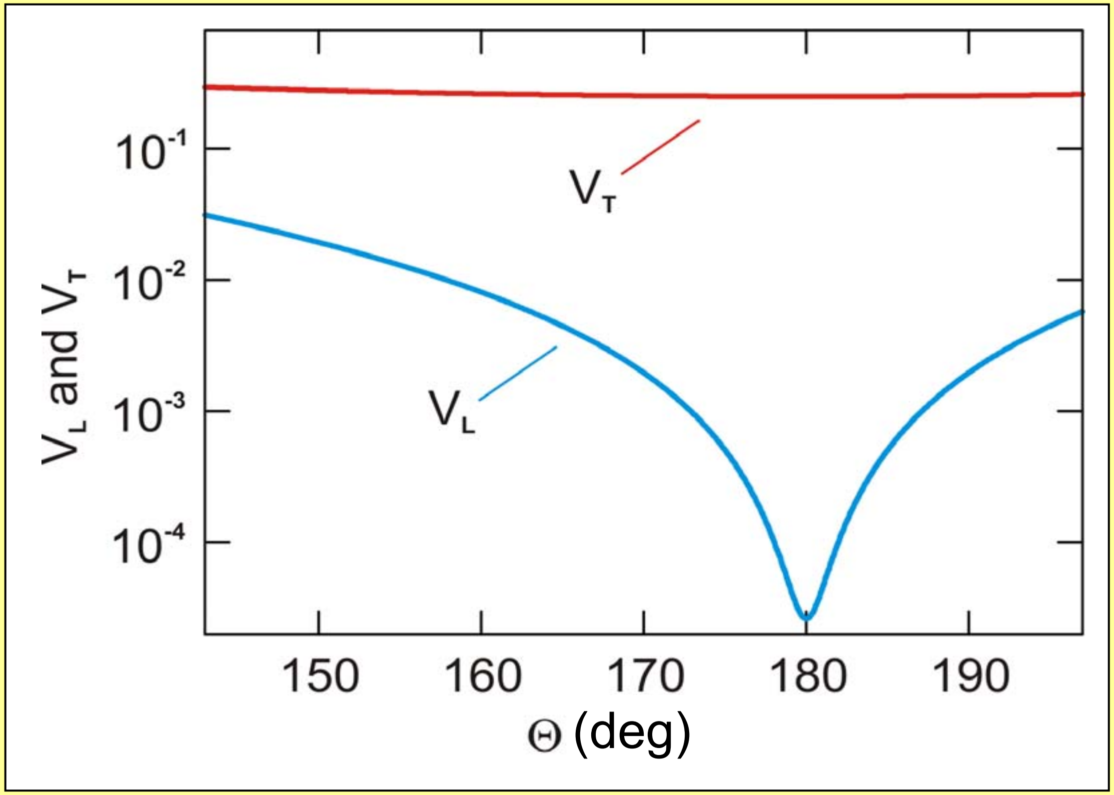

- Scattering at 180° is ideal for measuring transverse excitations: *M*1 enhanced

180° system at the S-DALINAC

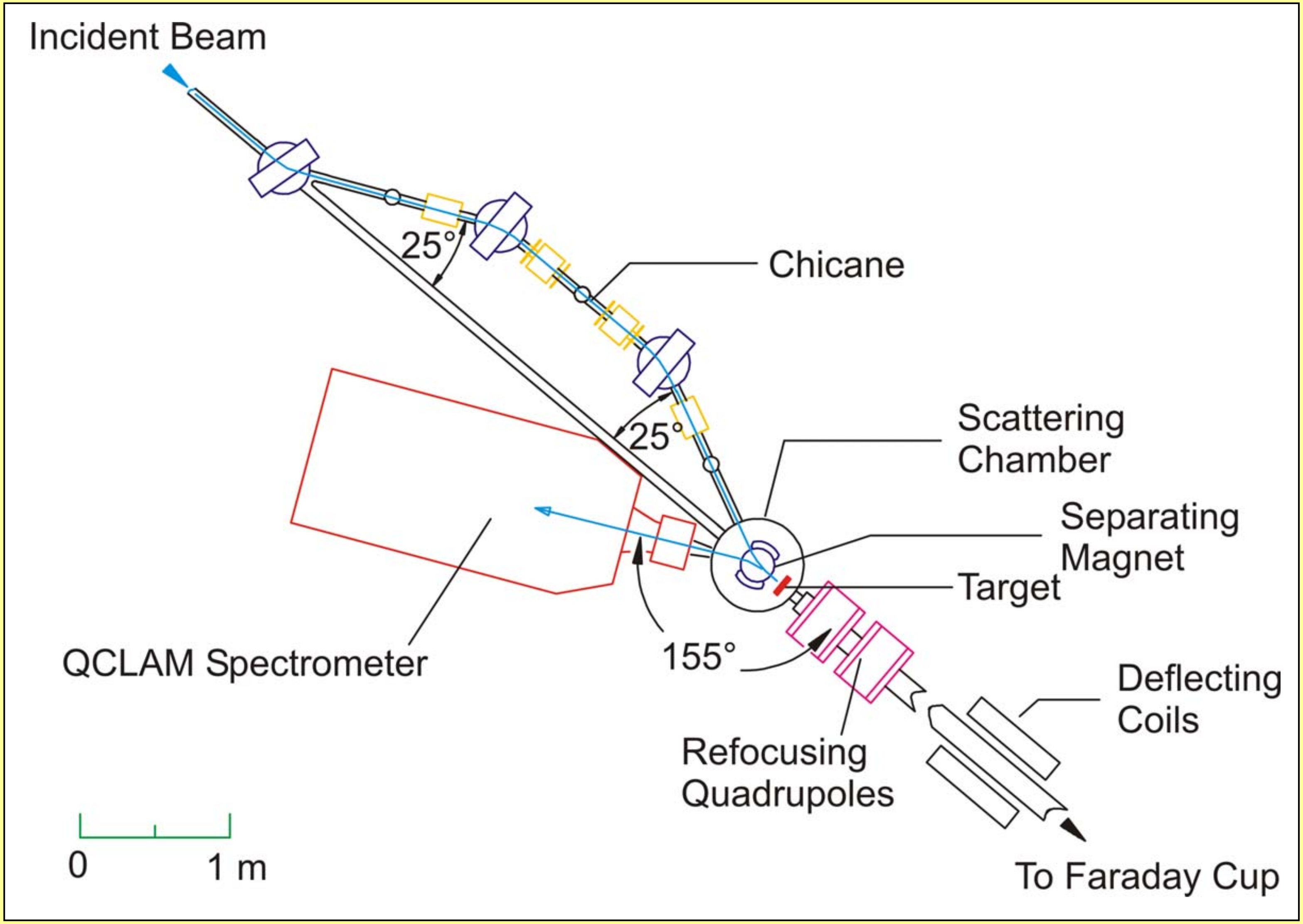

Decomposition of the spectra

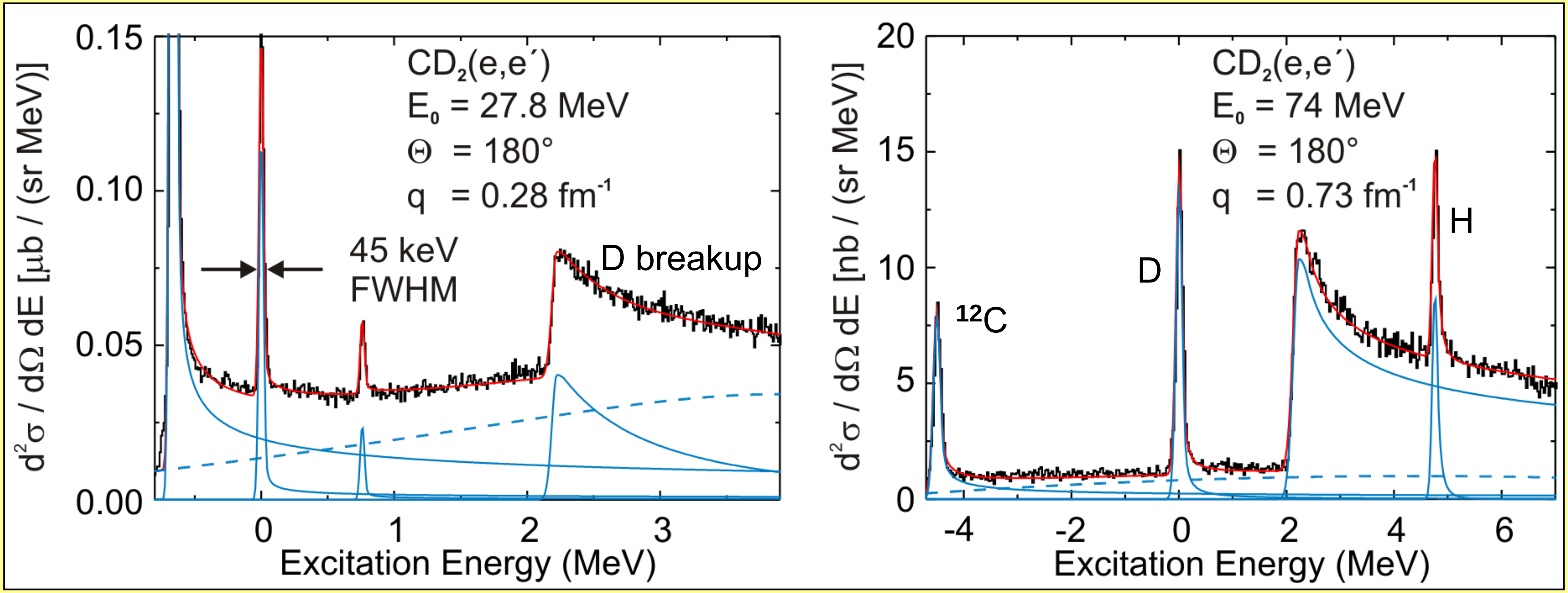

- Absolute and relative normalization agree within 5 - 6%

Comparison to potential model and EFT calculations

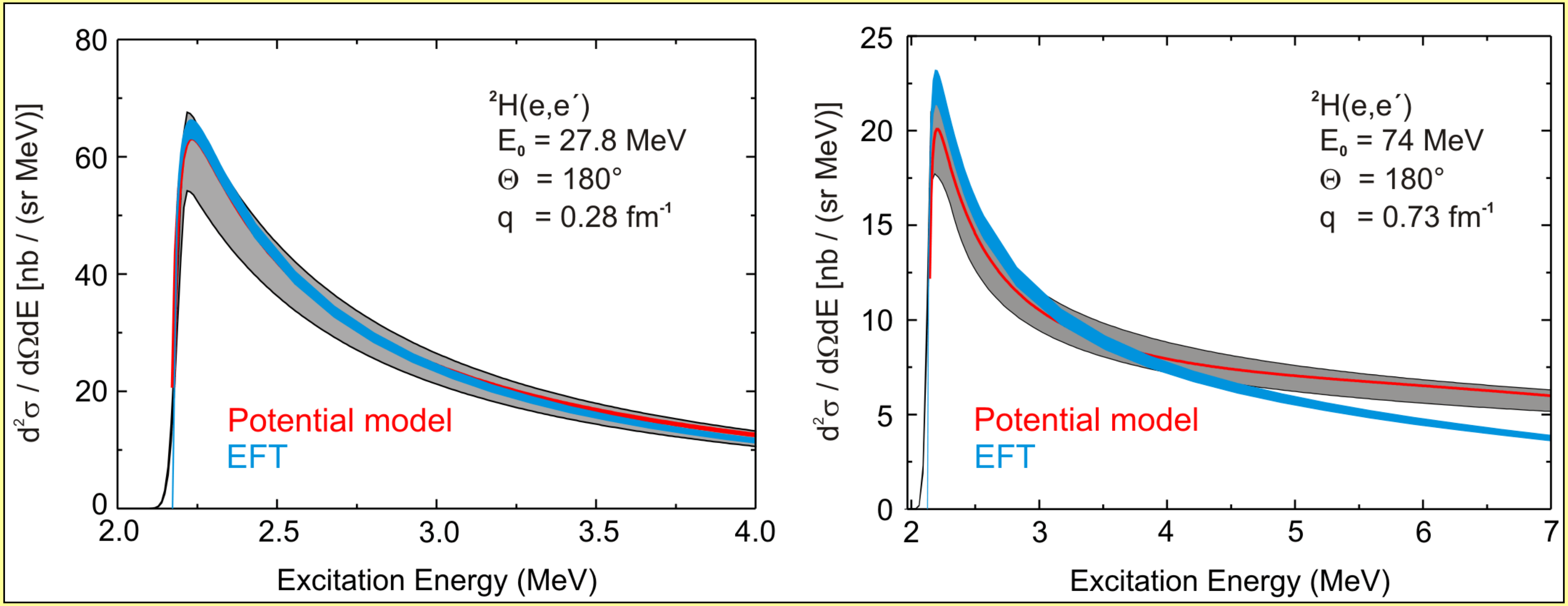

- Excellent agreement with potential model (H. Arenhövel)
- Deviations for EFT (H. Griesshammer) at higher *q*

Extraction of the astrophysical *np* → *d*γ cross section

- $\frac{d\sigma}{d\Omega}(\theta = 180^\circ, q) \sim F_T^2(q)$

- $B(M1, q) \sim \frac{1}{q^2} F_T^2(q)$

- For $q \to k$ (photon point) take q-dependence of B(M1,q) from elastic scattering → Γ_γ

- $\sigma(d\gamma \to np) \sim \frac{1}{E_\gamma^2} \frac{\Gamma_n \Gamma_\gamma}{(E_\gamma - E_R)^2 + \Gamma^2/4}$

- Detailed balance → $\sigma(np \to d\gamma)$

Importance for Big-Bang Nucleosynthesis

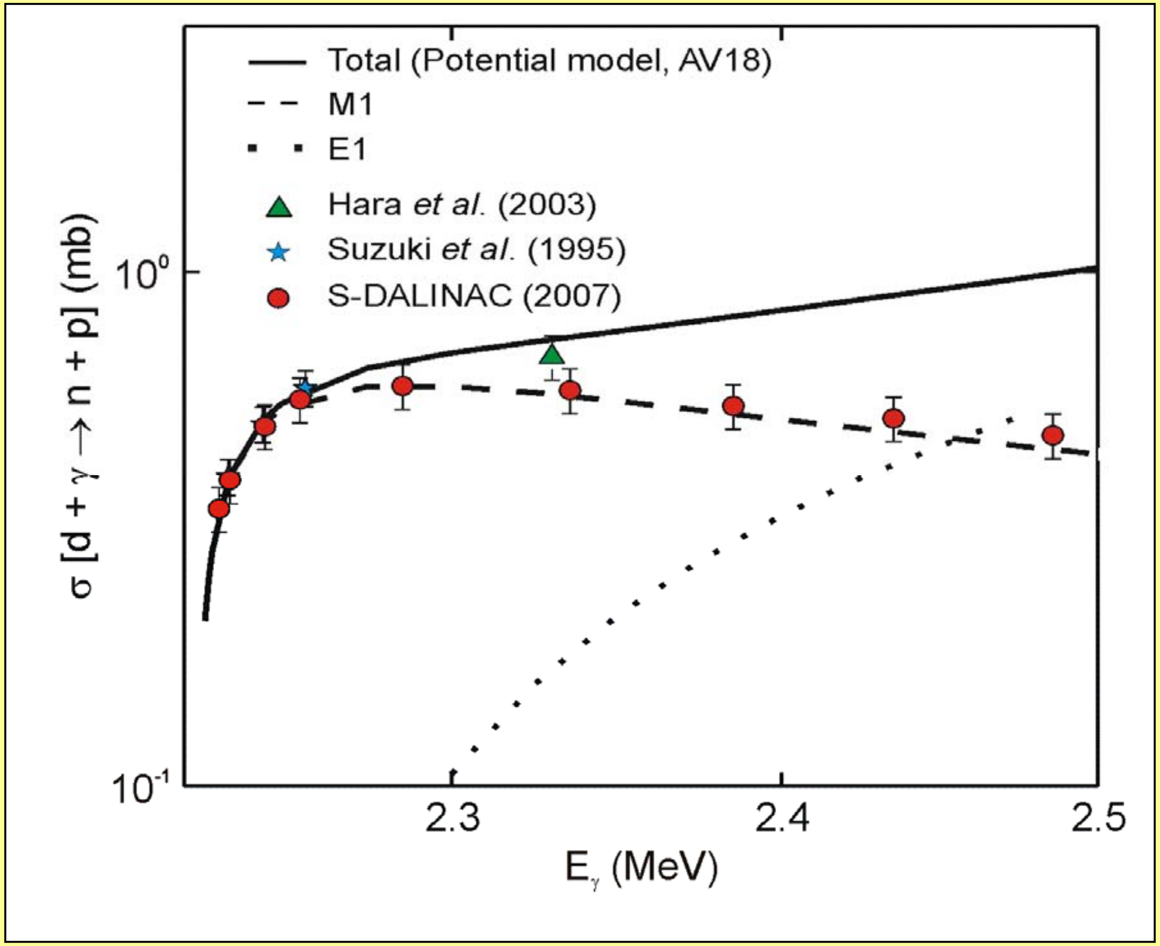

- BBN relevant energy window
- Precision test of modern theoretical models (potential model, EFT)

Summary and outlook

- Summary
  - 180° measurements of the *M*1 deuteron breakup
  - Precision test of modern theoretical models (potential model, EFT)
  - Excellent description of the data
  - Precise prediction for $p(n,\gamma)d$ cross section possible in the astrophysically relevant region
  - Latest BBN calculations use already EFT calculations
- Outlook
  - ^{9}Be(e,e´) under 180°

Possible role of ^{9}Be in the production of ^{12}C

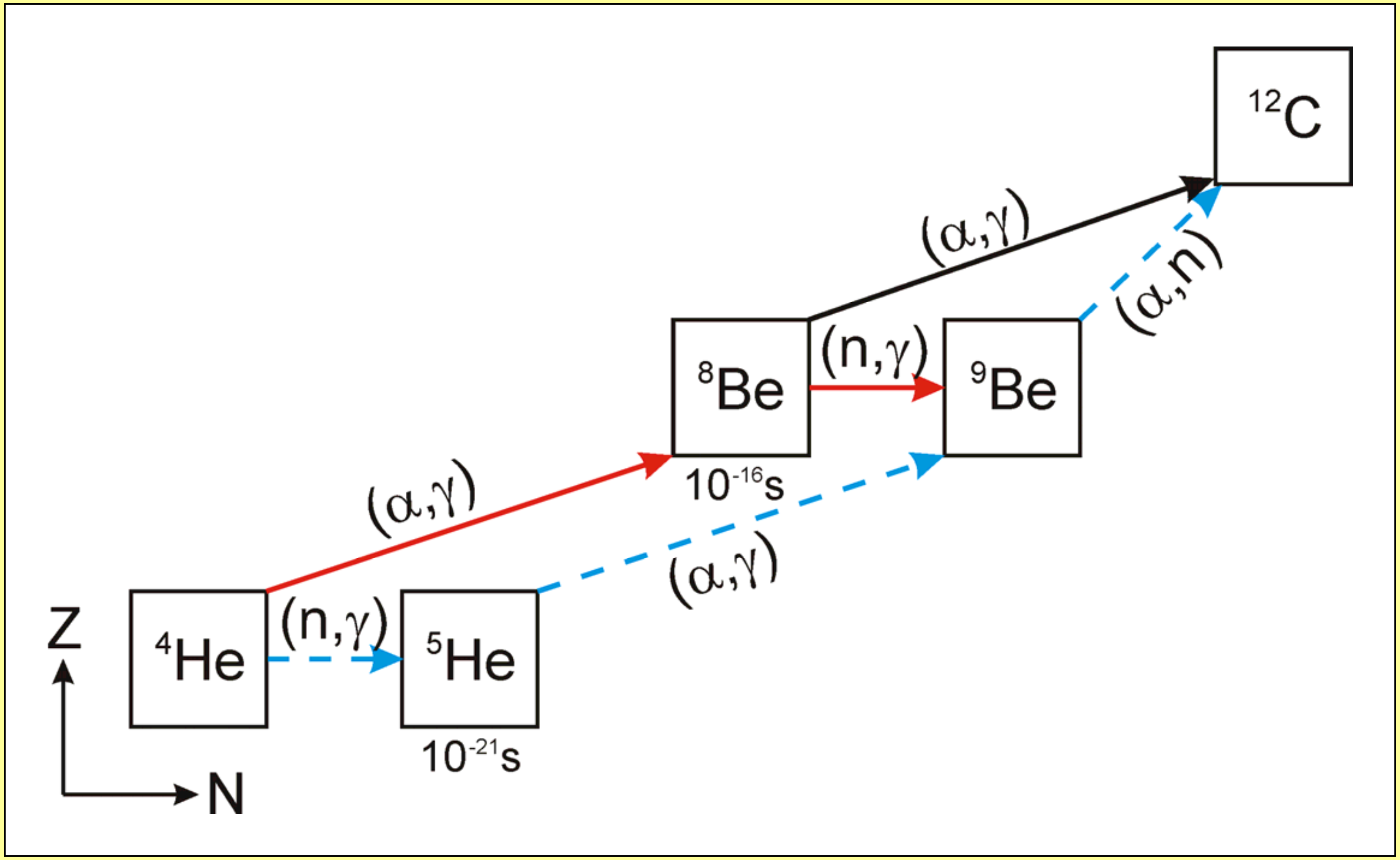

- In *n*-rich environment (core-collapse supernovae) this reaction path may provide an alternative route for building up the heavy elements and triggering the *r* process

O. Burda *et al.*, to be published

$J^\pi = ½^+$ state at threshold

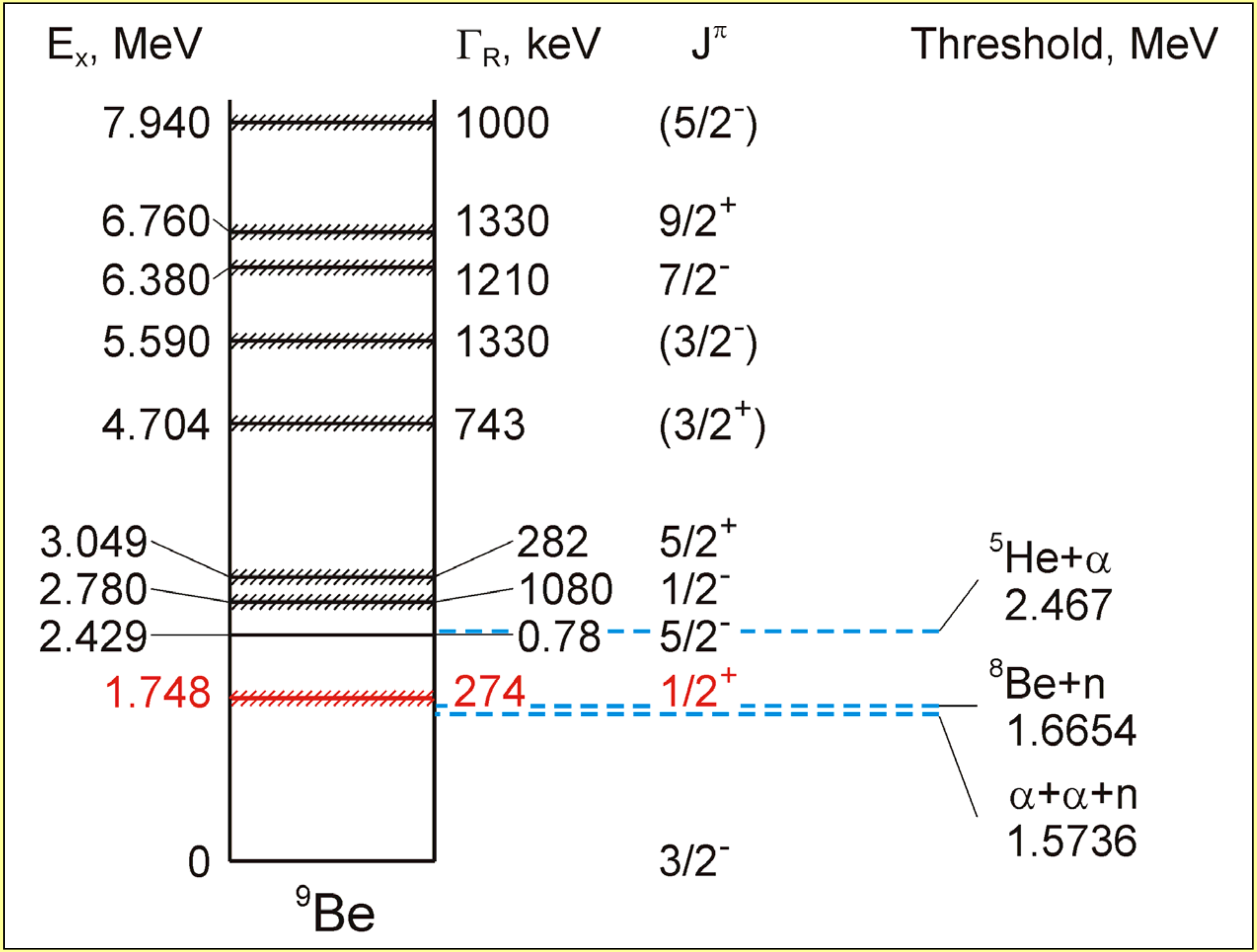

Lintott spectrometer

Detector system

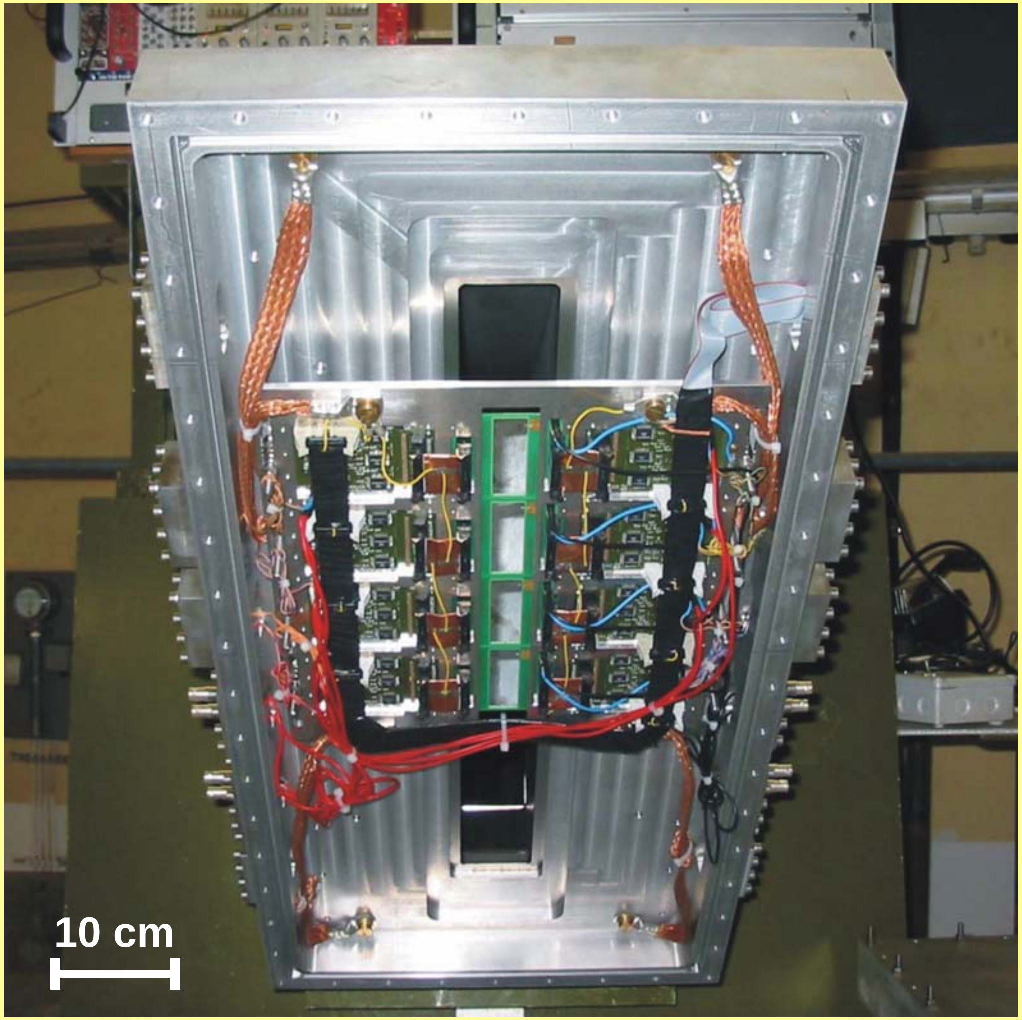

- Si microstrip detector system: 4 modules, each 96 strips with pitch of 650 μm
- Count rate up to 100 kHz
- Energy resolution 1.5×10^{-4}

Comparison: $^9Be(\gamma,n)$ and $^9Be(e,e')$

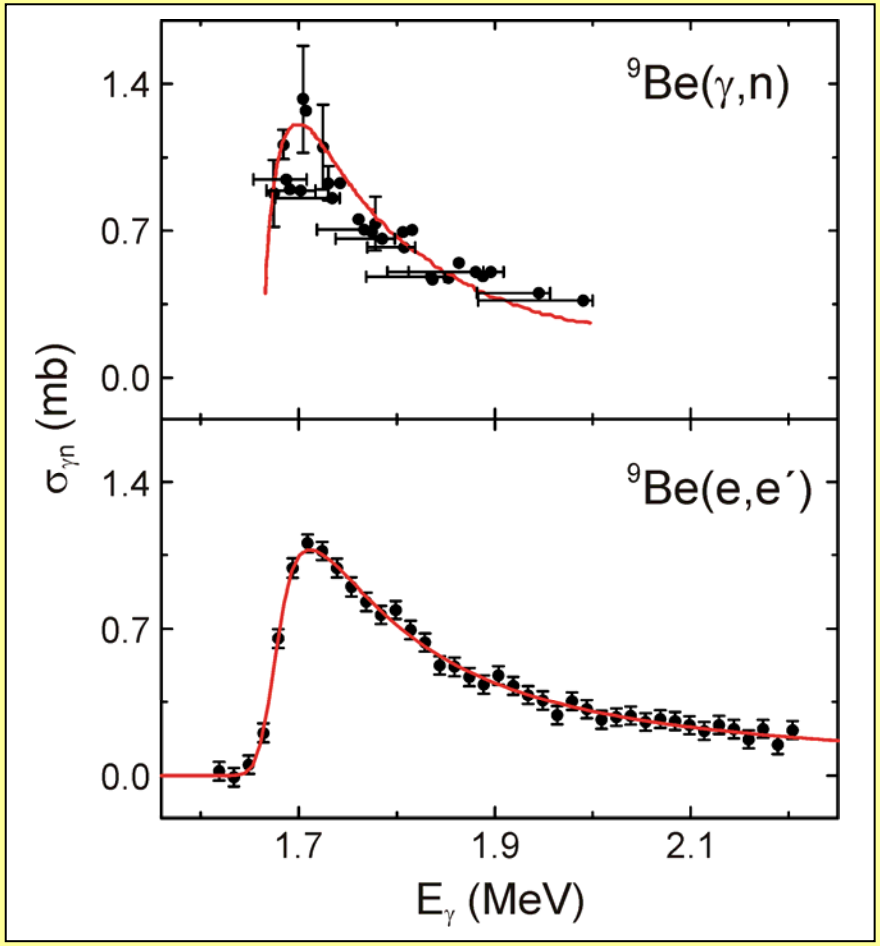

- Final values: E_x = 1.748(6) MeV and Γ = 274(8) keV of $J^\pi = ½^+$ resonance
  - For T_9 = 0.1 – 3 K this resonance determines exclusively $^4He(\alpha,\gamma)^8Be(n,\gamma)^9Be$ chain
  - Determined reaction rate differs up to 20% from adopted values

Form factor of the $J^{\pi} = ½^{+}$ state

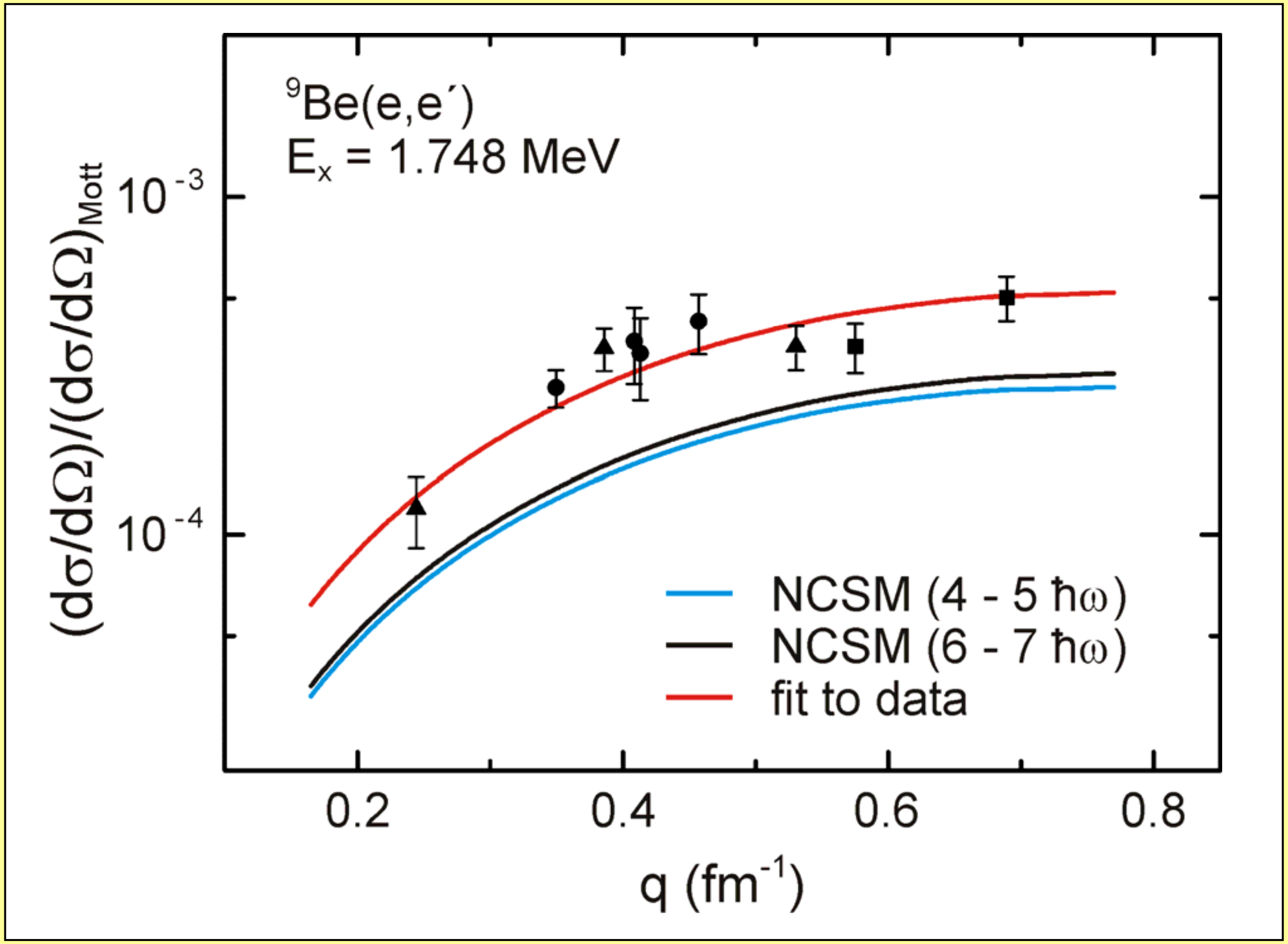

- NCSM: correct *q* dependence but difference in magnitude compared to the data (C. Forssén)
- B(*C*1) ≠ B(*E*1) at photon point $k = q$
  → violation of Siegert theorem ?

Hoyle state in ^{12}C

- Astrophysical motivation
- Experiment
  - High-resolution electron scattering
- Nuclear structure
  - Structure of the Hoyle state: a “BEC” ?
  - Higher lying 0^+ and 2^+ states
  - Comparison with FMD and α-cluster model predictions
- Summary and outlook

M. Chernykh, H. Feldmeier, T. Neff, P. von Neumann-Cosel and A. Richter, PRL 98, 032501 (2007)

Motivation: triple alpha process

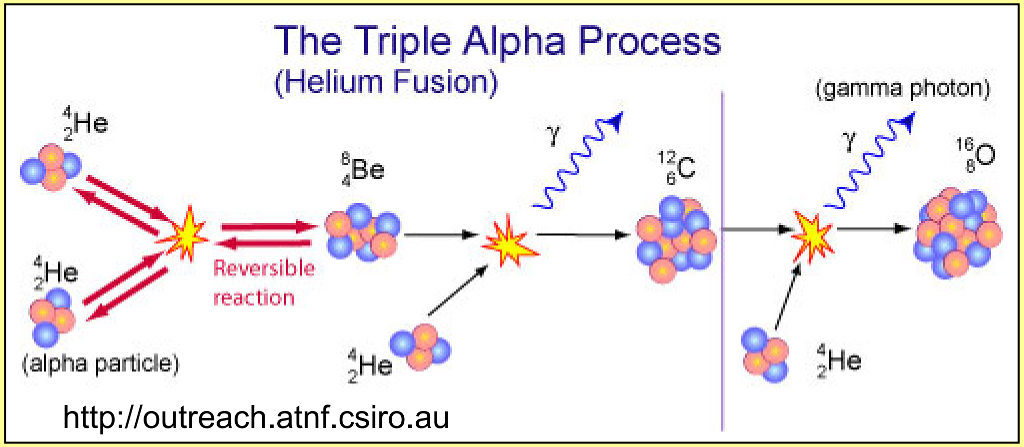

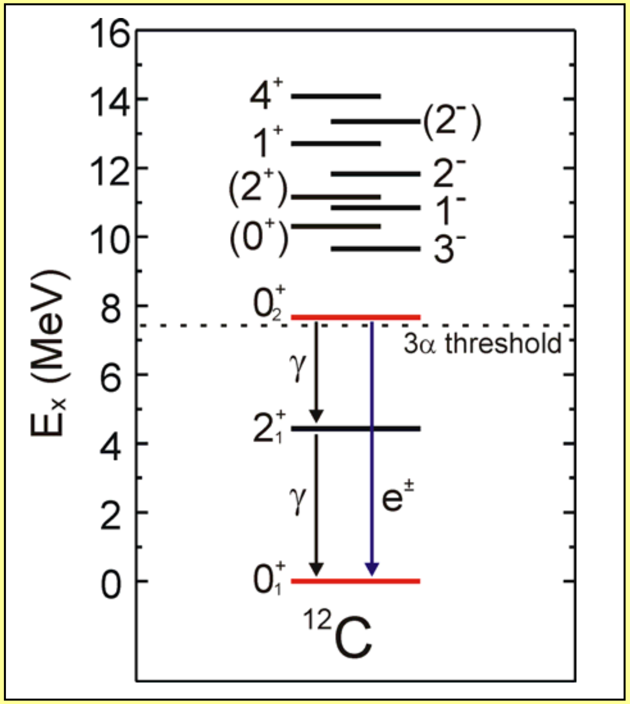

- Reaction rate:

$$\Gamma_{rad} = \Gamma_\gamma + \Gamma_\pi = \frac{\Gamma_\gamma + \Gamma_\pi}{\Gamma} \cdot \frac{\Gamma}{\Gamma_\pi} \cdot \Gamma_\pi$$

$$r_{3\alpha} \propto \Gamma_{rad} \exp\left(-\frac{Q_{3\alpha}}{kT}\right)$$

S.M. Austin, NPA 758, 375c (2005)

- Electron scattering → M(E0) → extraction of Γ_π
- 0^+_1 and 0^+_2 (7.654 MeV) states in ^{12}C
  - Density distributions
  - Model predictions

Measured spectra

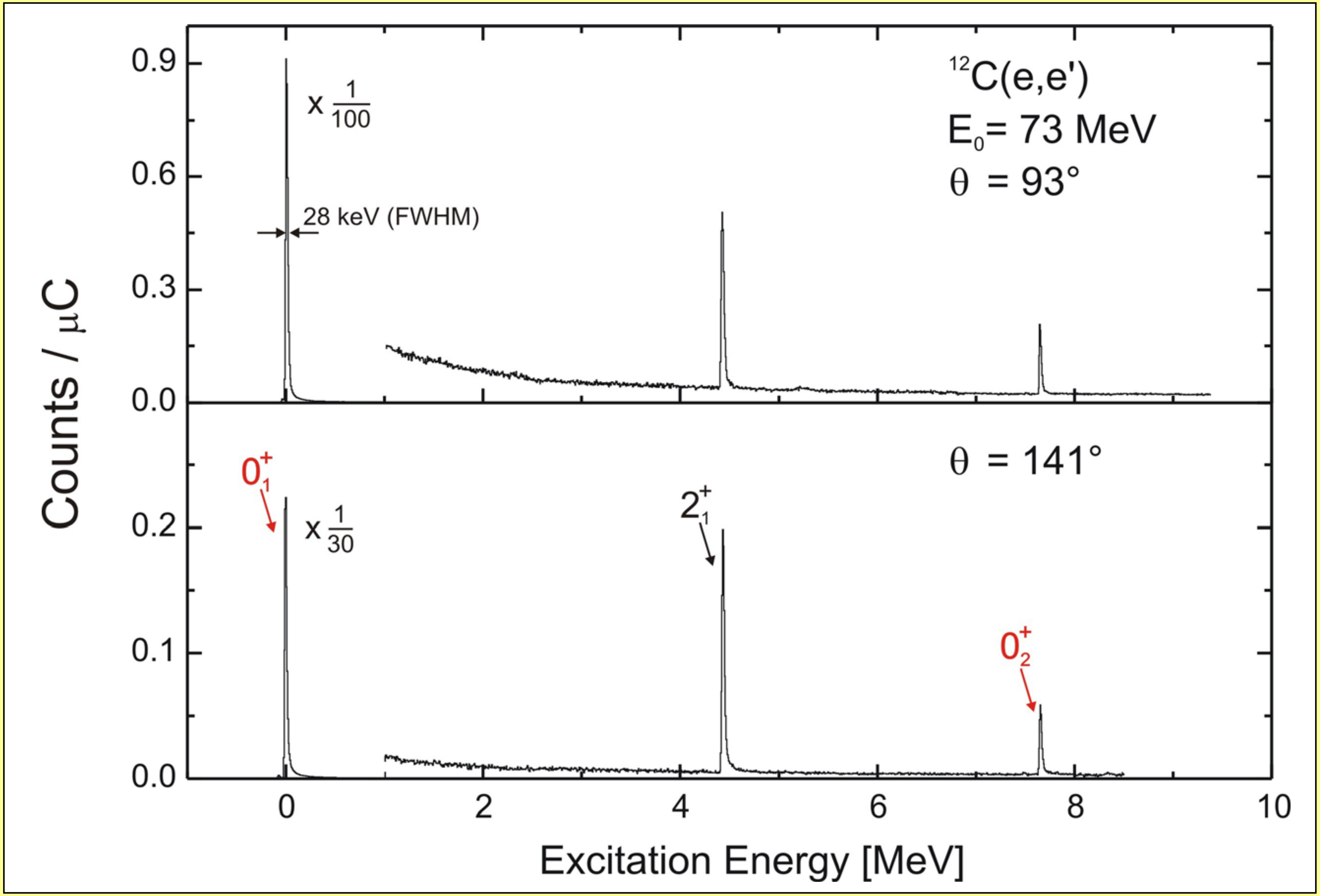

Theoretical approaches: FMD model

- Antisymmetrized A-body state

$$|Q\rangle = \mathcal{A}(|q_1\rangle \otimes |q_2\rangle \otimes \ldots \otimes |q_A\rangle)$$

  – Single-particle states

$$\langle \mathbf{x}|q\rangle = \sum_i c_i \exp\Big[-\frac{(\mathbf{x}-\mathbf{b}_i)^2}{2a_i}\Big] \otimes |\chi_i^\uparrow, \chi_i^\downarrow\rangle \otimes |\xi\rangle$$

  – Gaussian wave packets in phase space (a_i is width, complex parameter $\mathbf{b}_i$ encodes mean position and mean momentum), spin is free, isospin is fixed

  – Describes α-cluster states as well as shell-model–like configurations

- UCOM interaction

  – Derived form the realistic Argonne V18 interaction

  – Adjusted to reproduce binding energies and charge radii of some “closed-shell” nuclei

Theoretical approaches: α-cluster and "BEC" models

- α-cluster model
  - FMD wave function restricted to α-cluster triangle configurations only

- "BEC" model
  - System of 3 ^{4}He nuclei in 0s state (like α condensate)
  - Hoyle state is a "dilute gas" of α particles

- Volkov interaction
  - Simple central interaction
  - Parameters adjusted to reproduce α binding energy, radius, $\alpha - \alpha$ scattering data and ground state energy of ^{12}C
  - Only reasonable for ^{4}He, ^{8}Be and ^{12}C nuclei

^{12}C densities

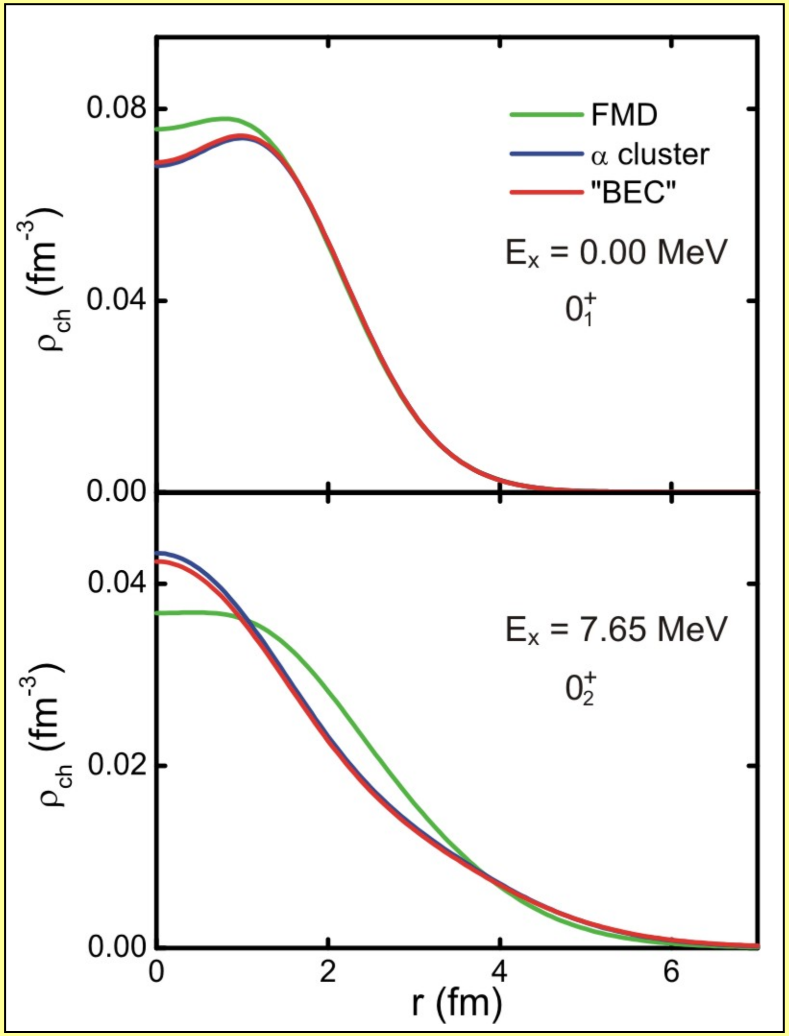

- Ground state density can be tested via elastic form factor

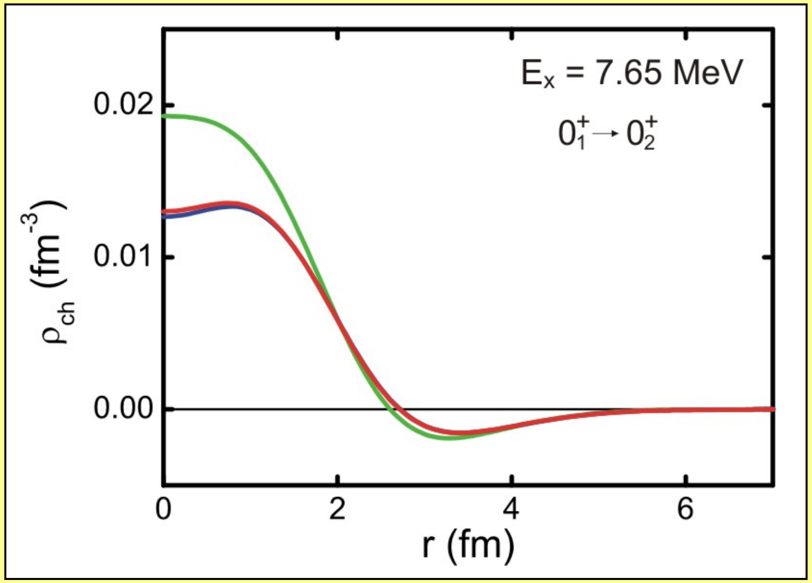

- Transition density can be tested via transition form factor

- Electron scattering as test of theoretical predictions

Elastic form factor

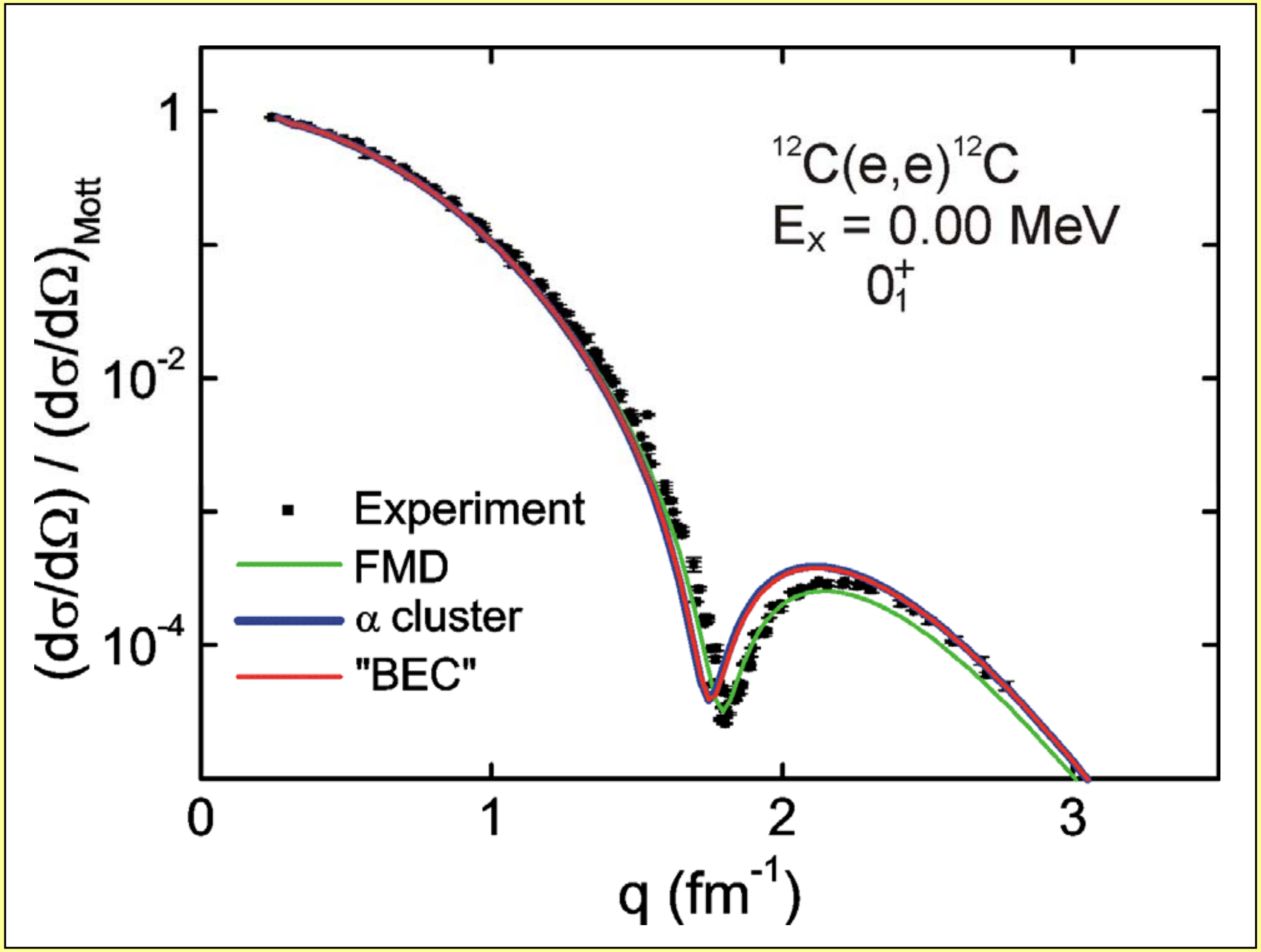

- H. Crannell, data compilation
- Described well by FMD

Transition form factor to the Hoyle state

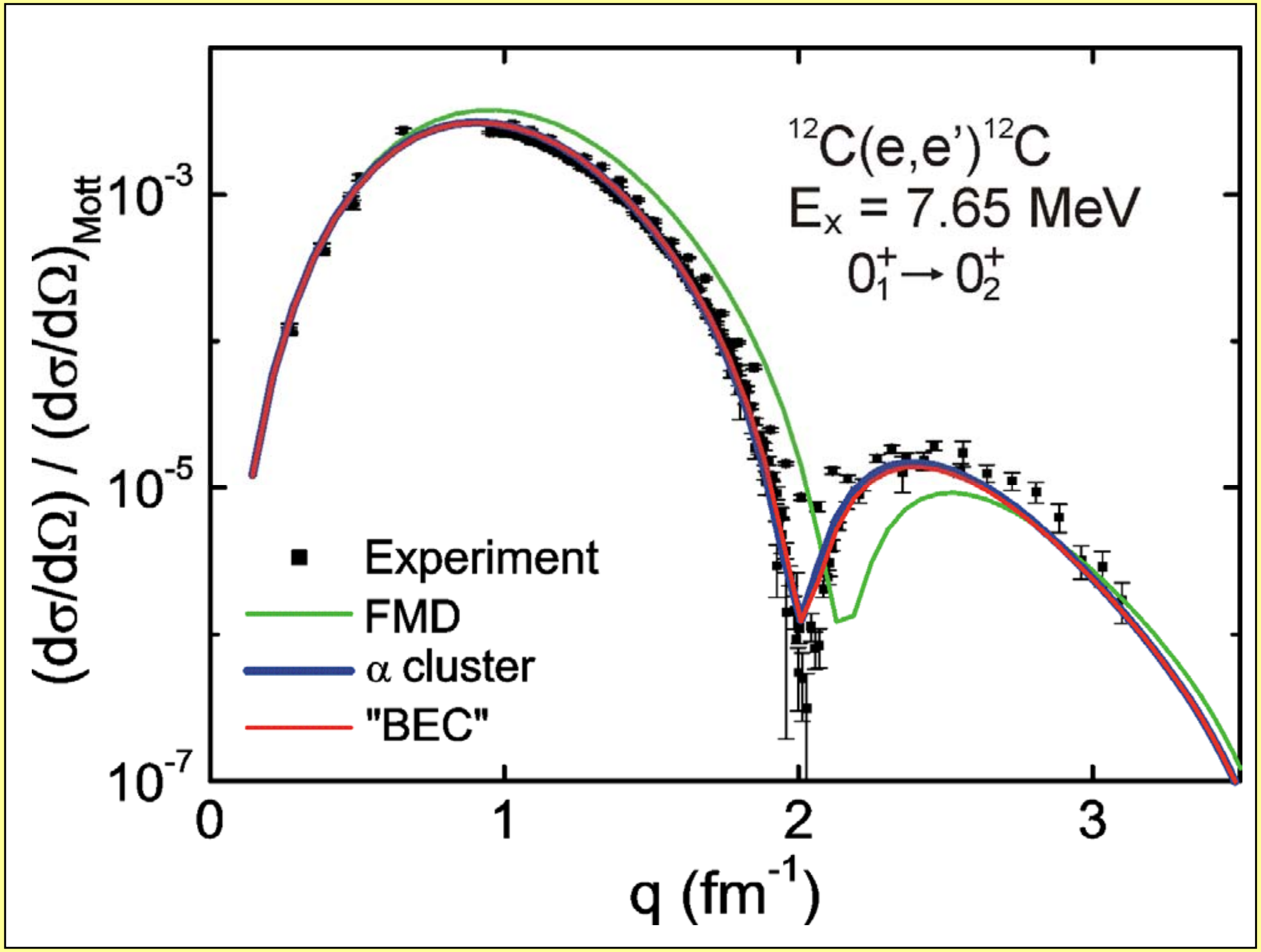

- H. Crannell, data compilation
- Described better by α-cluster models
- FMD might be improved by taking α-α scattering data into account

What is actual structure of the Hoyle state ?

- Overlap with FMD basis states

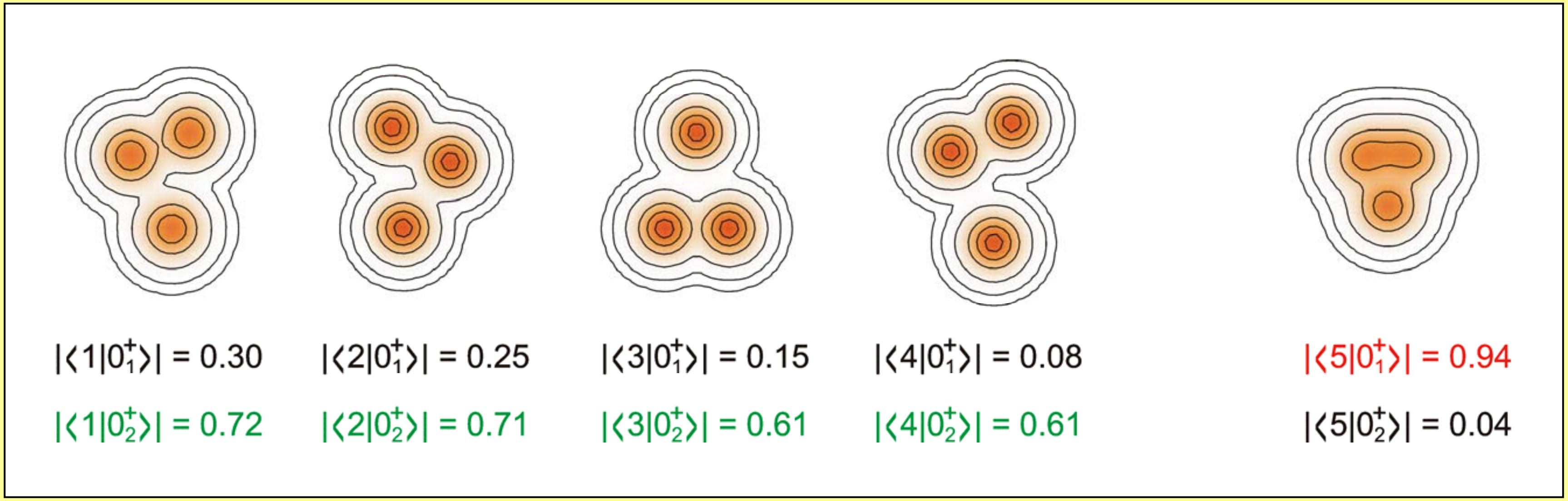

- In the FMD and α-cluster model the leading components of the Hoyle state are cluster-like and resemble ^{8}Be + ^{4}He configurations

- But in the “BEC” model the relative positions of α clusters should be uncorrelated

Summary and outlook

- Summary
  - Hoyle state is not a true Bose-Einstein condensate
  - $^{8}Be + \alpha$ structure
- Outlook
  - ^{12}C: 0_3^+ and 2_2^+ states
  - ^{16}O: broad 0^+ state at 14 MeV
  - Γ_π for decay of the Hoyle state

Supernova inelastic neutrino-nucleus cross section

(i) Important for

- *r* process
- ν process
- ν detectors
- Supernova physics
  - Opacities and thermalization during collapse phase
  - Delayed explosion mechanism
  - Explosive nucleosynthesis

(ii) ν scattering so far not included in supernova modeling

K. Langanke, G. Martínez-Pinedo, P. von Neumann-Cosel and A. Richter, PRL 93, 202501 (2004)

Supernova dynamics and explosive nucleosynthesis

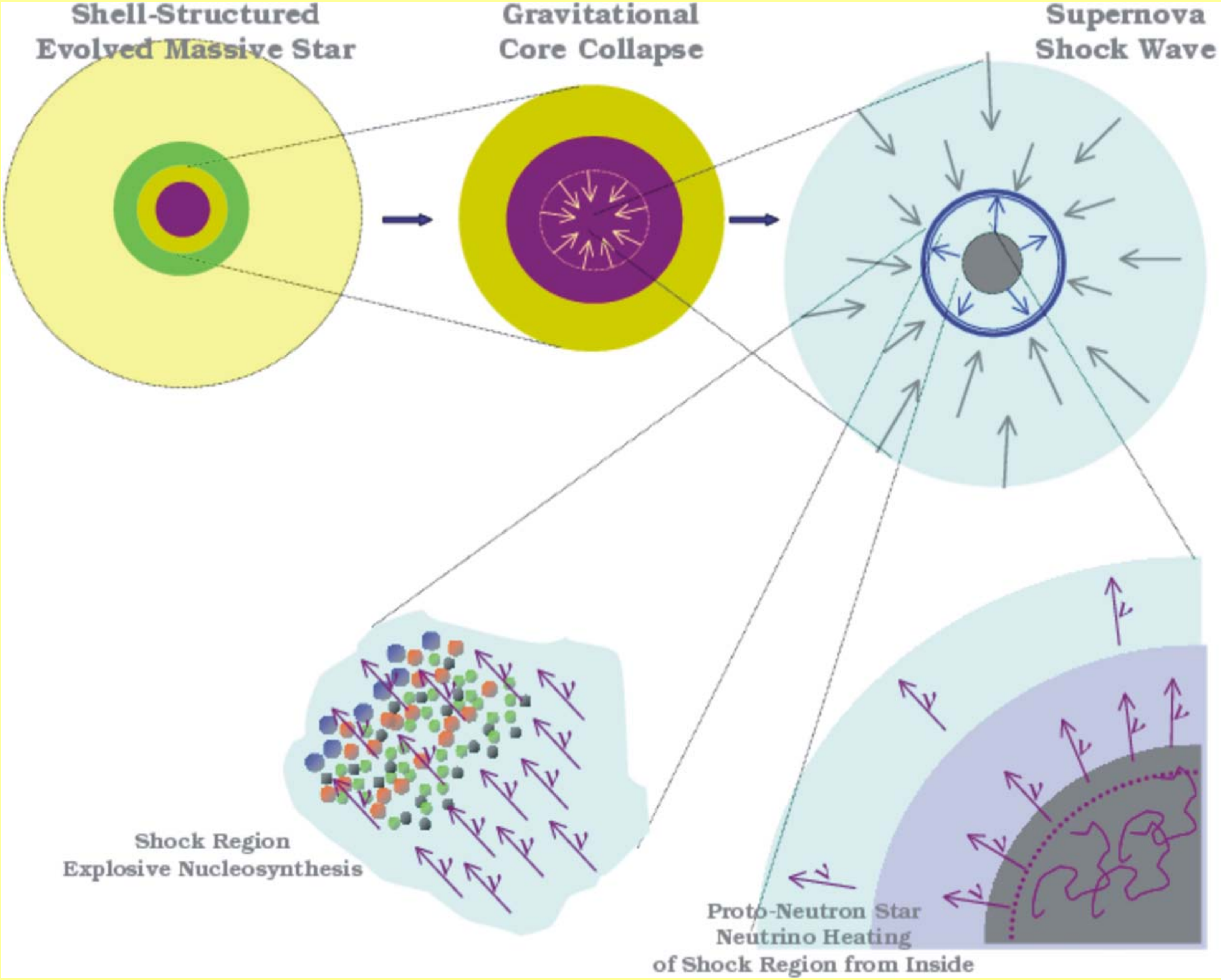

Neutrino interactions during the collapse

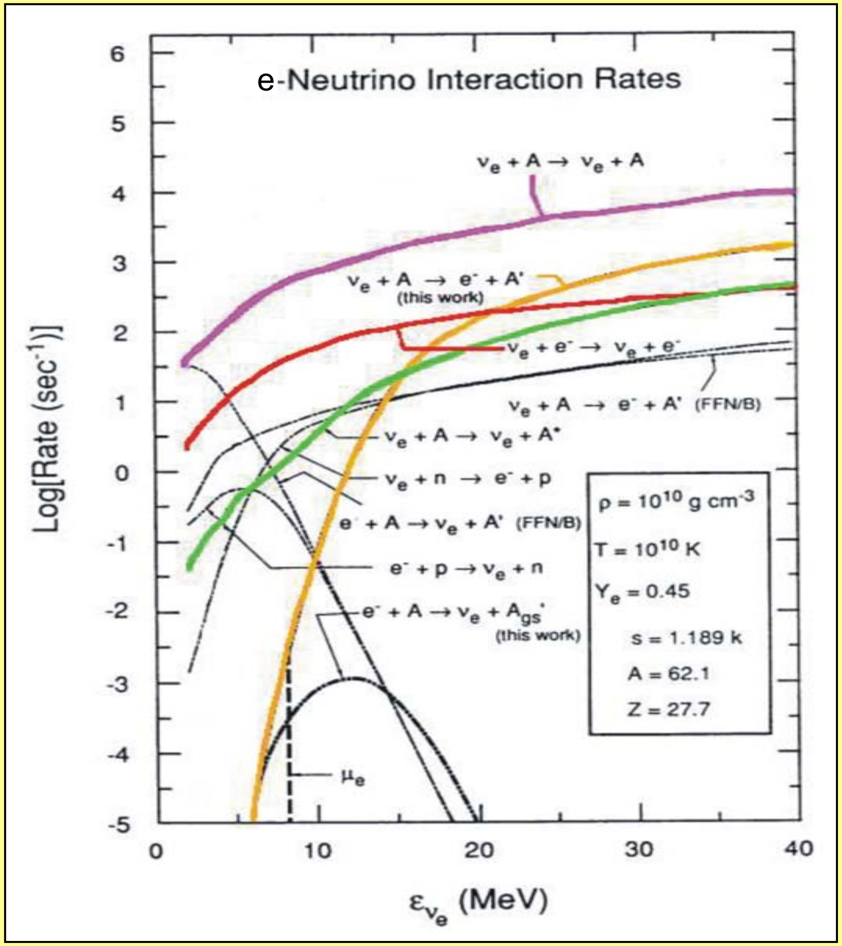

- Elastic scattering:
  $\nu + A \Leftrightarrow \nu + A$ (trapping)
- Absorption:
  $\nu_e + (N, Z) \Leftrightarrow e^- + (N-1, Z+1)$
- ν-e scattering:
  $\nu + e^- \Leftrightarrow \nu + e^-$
- Inelastic ν-nucleus scattering:
  $\nu + A \Leftrightarrow \nu + A^*$

- Inelastic neutrino-nucleus interactions had not been included in collapse simulations

S.W. Bruenn and W.C. Haxton, Ap. J. 376, 678 (1991); based on results for ^{56}Fe

Experimental information

- Direct: ^{12}C, $J^{\pi} = 1^{+}$, T = 1, E_x = 15.11 MeV

- Indirect: low energy ν's → low multipolarity transitions

- Idea: extract GT_0 strength in nuclei from *M*1 response

$$T(M1)_{IV} = \sqrt{\frac{3}{4\pi}} \sum_i [\vec{l}_i \vec{t}_{zi} + (g_s^p - g_s^n) \vec{s}_i \vec{t}_{zi}] \mu_N$$

$$\updownarrow$$

$$T(GT_0) = 2 \sum_i [\vec{s}_i \vec{t}_{zi}]$$

ν-nucleus scattering cross section

- $\sigma(i \rightarrow f) = \frac{G_F^2}{\pi}(E_\nu - E_x)^2 B(GT_0)$

- $B(GT_0)$ from isovector *M*1 strength
  - Orbital and isoscalar pieces small

- Test cases: ^{50}Ti, ^{52}Cr, ^{54}Fe with precision data on *M*1 strength from (e,e´) experiments

^{52}Cr: experiment vs. "state of the art" SM calculations

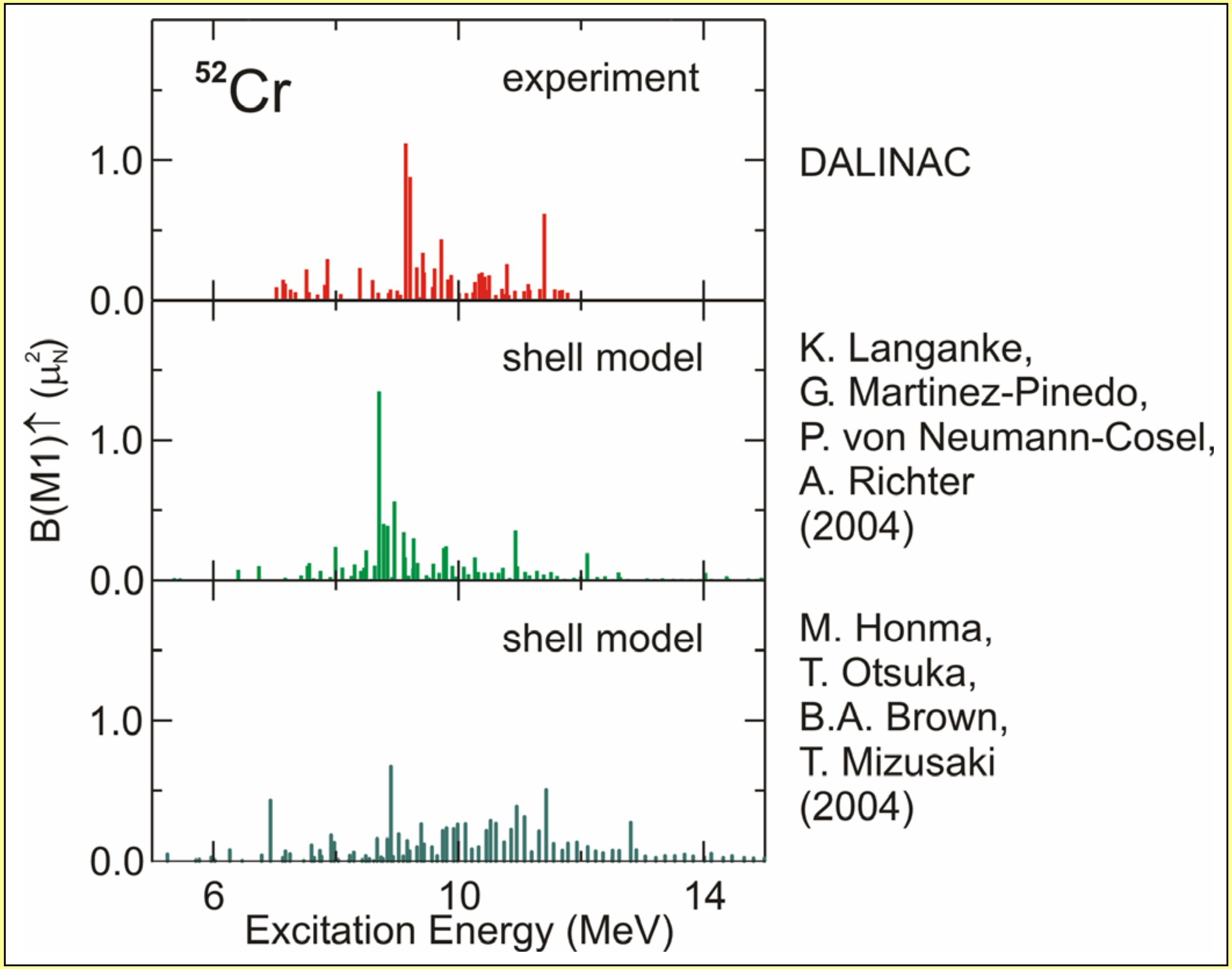

- Still significant differences between different effective interactions
- Role of orbital strength ?

Role of orbital *M*1 strength

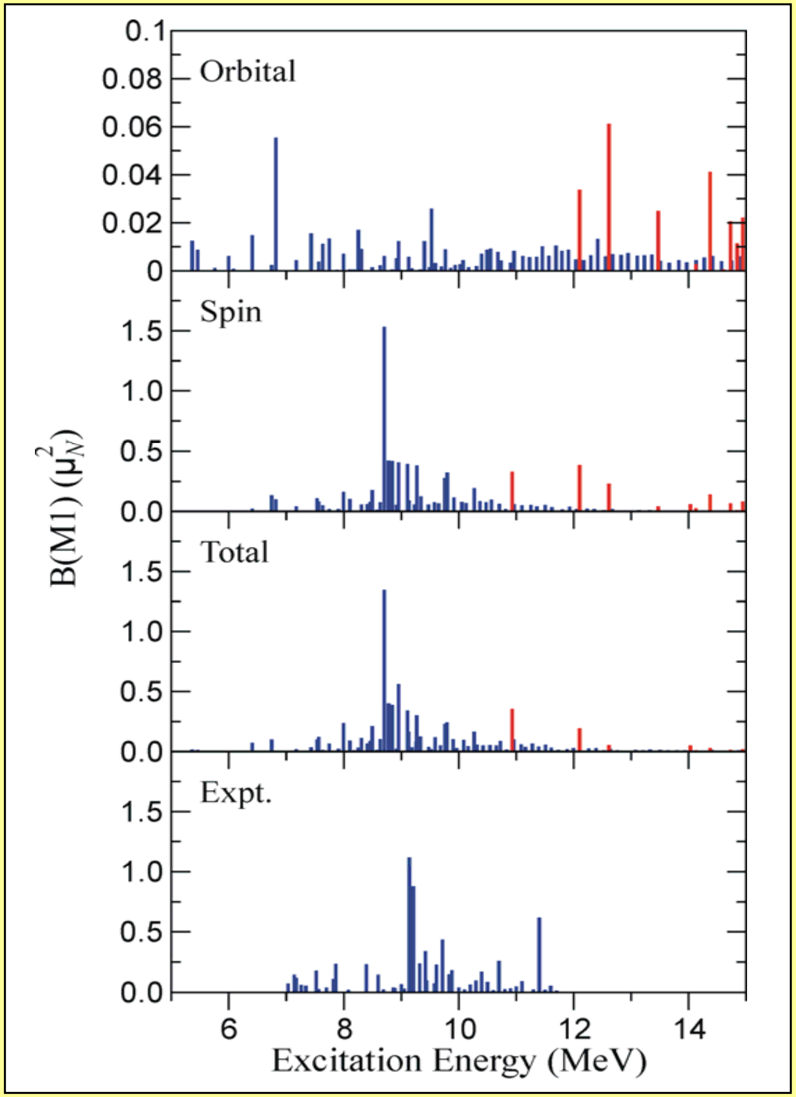

- Orbital *M*1 strength is negligible

K. Langanke *et al.*, PRL 93, 202501 (2004)

Differential ν nucleus cross section

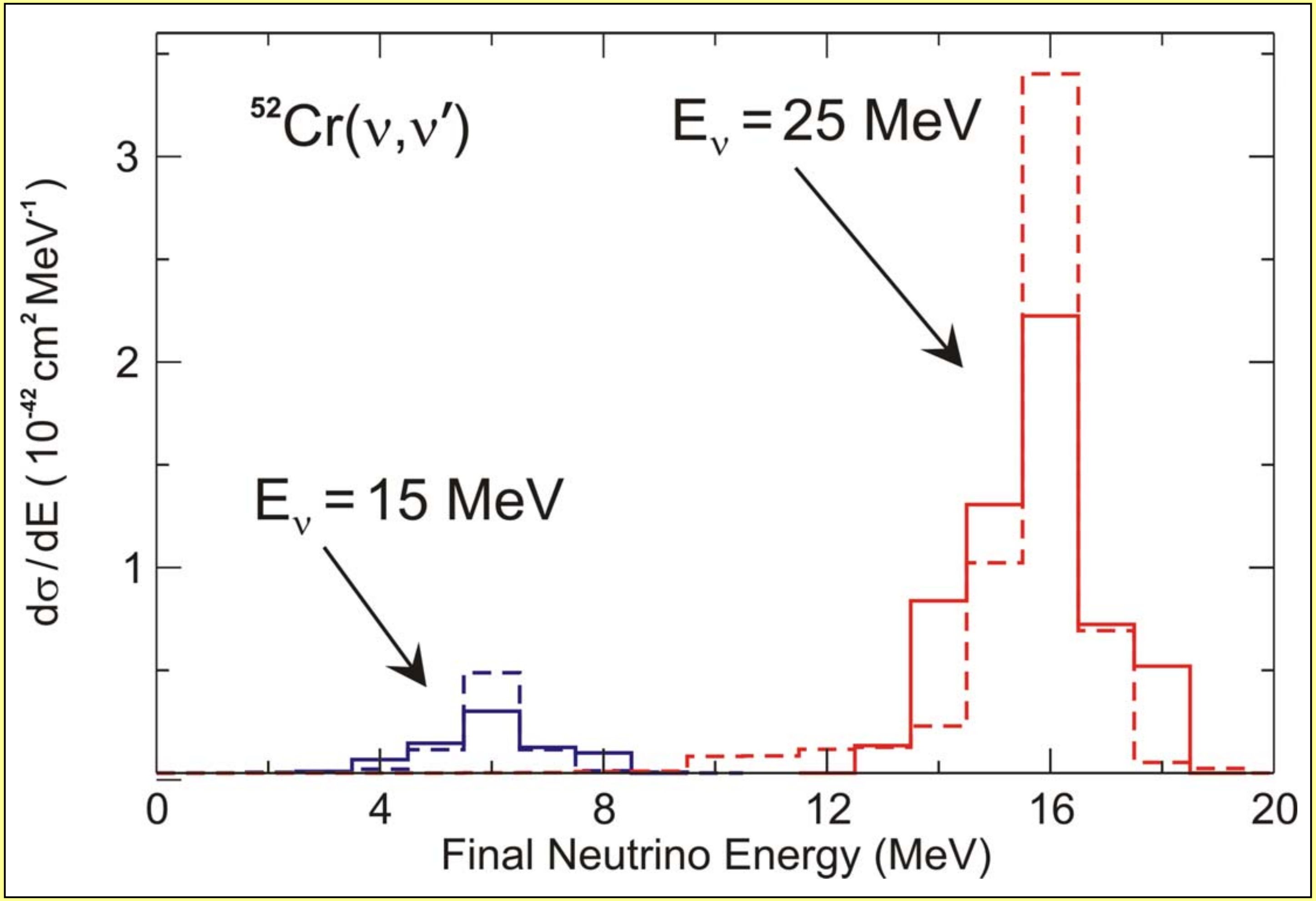

- E_ν(final) = $E_\nu - E_X(GT_-)$
- Good agreement between experiment and theory → shell-model results can be used for systematic treatment

Influence on neutrino spectra

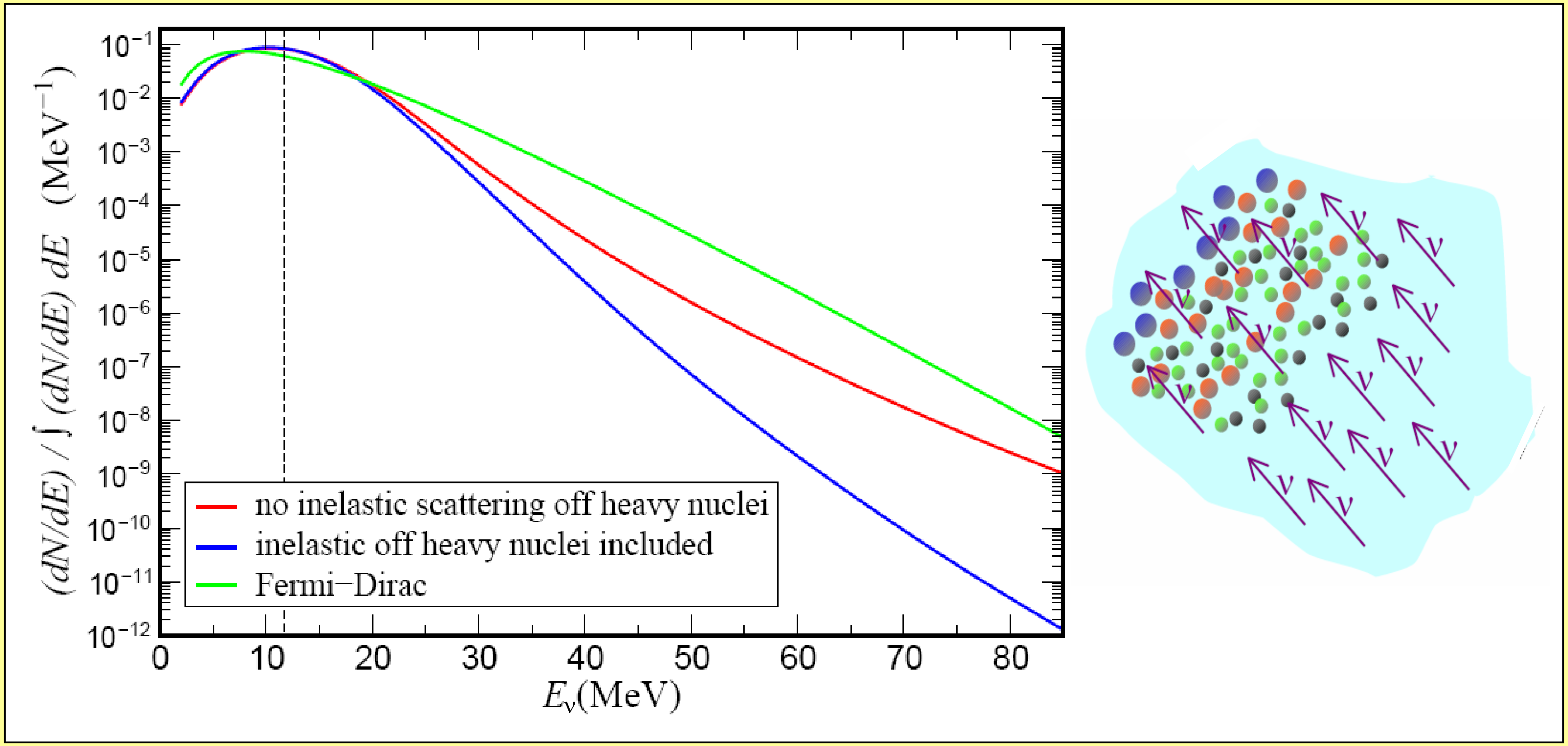

- Spectrum of the initial ν_e burst is affected by the inclusion of inelastic neutrino scattering on nuclei (B. Müller *et al.*)
- What is the impact on supernova neutrino detection ?

Impact on typical detector materials

Material	$\langle\sigma\rangle$ $(10^{-42}$ cm$^2)$ Without INNS	With INNS	Change
e	0.110	0.106	3%
d	5.36	4.92	8%
^{12}C	0.080	0.050	37%
^{16}O	0.0128	0.0053	58%
^{40}Ar	15.1	13.4	11%
^{56}Fe	7.5	6.2	17%
^{208}Pb	124.5	103.3	17%

- This correction has to be included if one wants to extract information on supernova dynamics
- At later times (relevant for nucleosynthesis) ν spectra are unchanged as all nuclei are dissociated

Neutrino nucleosynthesis of exotic, odd-odd nuclei ^{138}La and ^{180}Ta

- Motivation
- Neutrino nucleosynthesis of ^{138}La and ^{180}Ta
- High resolution measurement of GT strength
- Results and conclusions

A. Byelikov *et al.*, PRL 98, 082501 (2007)

Exotic nuclides

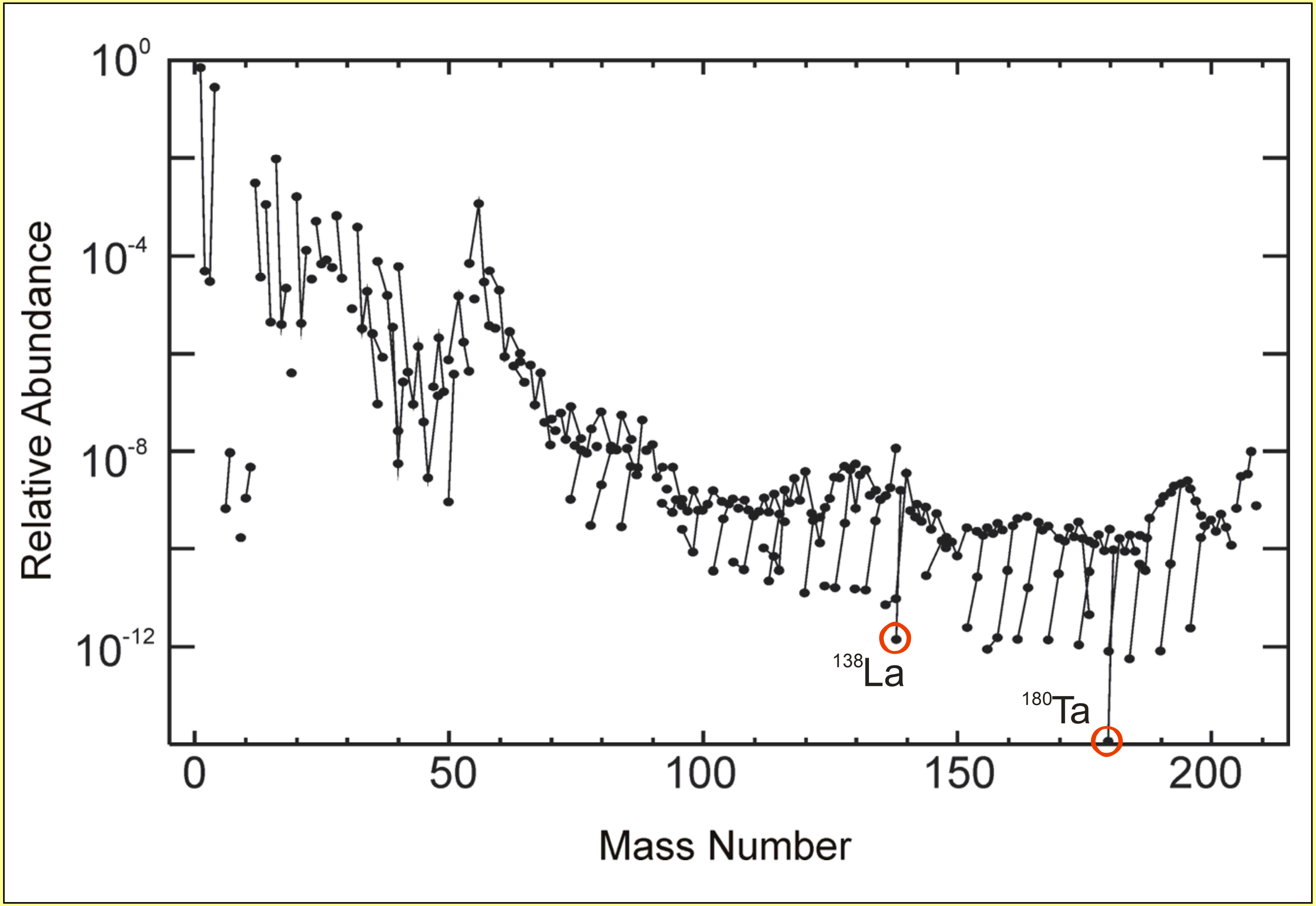

Nucleosynthesis of ^{138}La

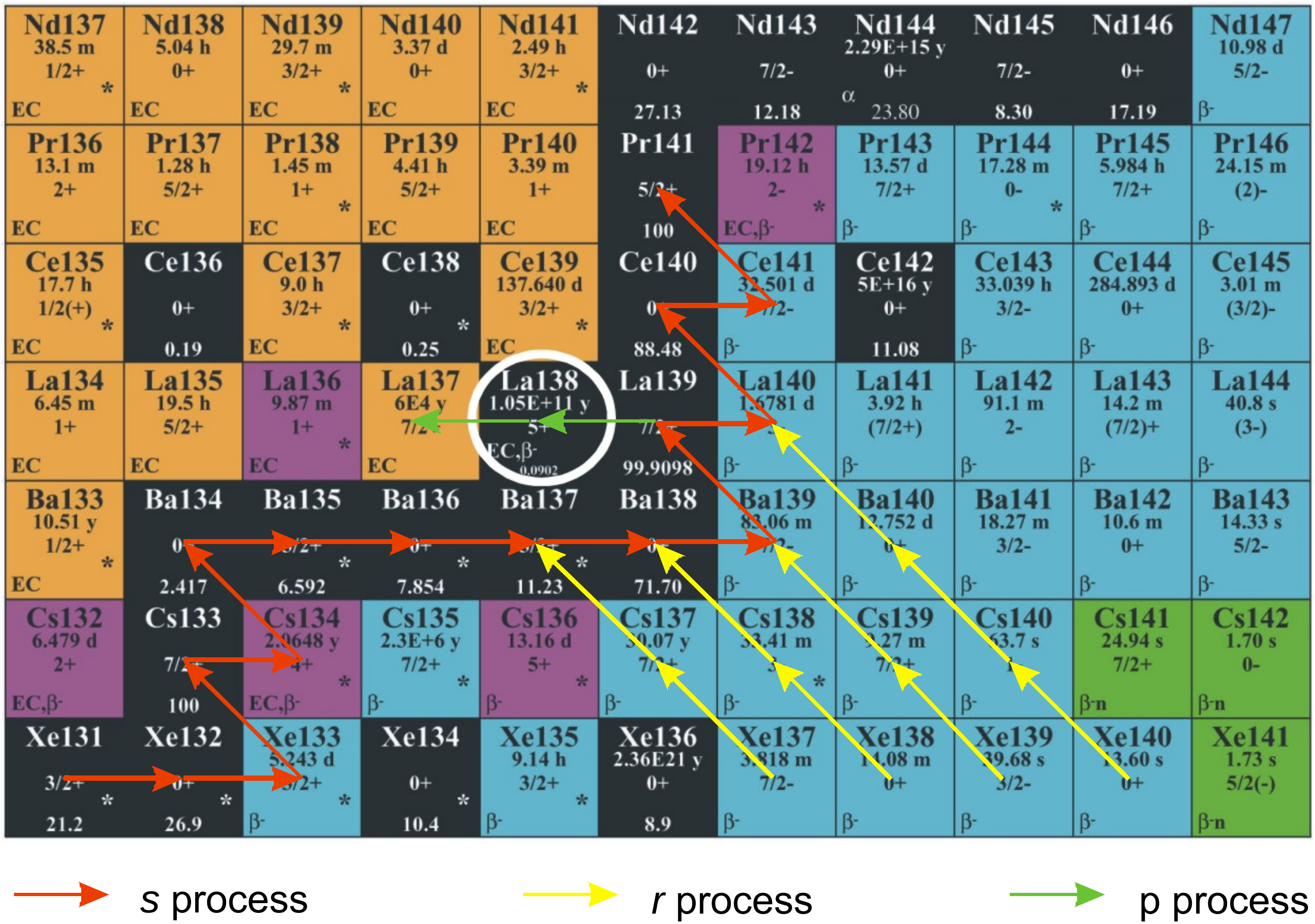

Production through neutrino process

- Neutral current reactions: $^{139}La(\nu,\nu' n)^{138}La$
  $^{181}Ta(\nu,\nu' n)^{180}Ta$

- Charged current reactions: $^{138}Ba(\nu_e,e^-)^{138}La$
  $^{180}Hf(\nu_e,e^-)^{180}Ta$

- Complete stellar evolution in massive stars → realistic distribution of seed nuclei and for core properties

  T. Rauscher *et al.*, Ap. J. 576, 323 (2002)

- Supernova calculations with improved RPA input for ν-nucleus reactions

  A. Heger *et al.*, PLB 606, 285 (2005)

Different production processes of ^{138}La

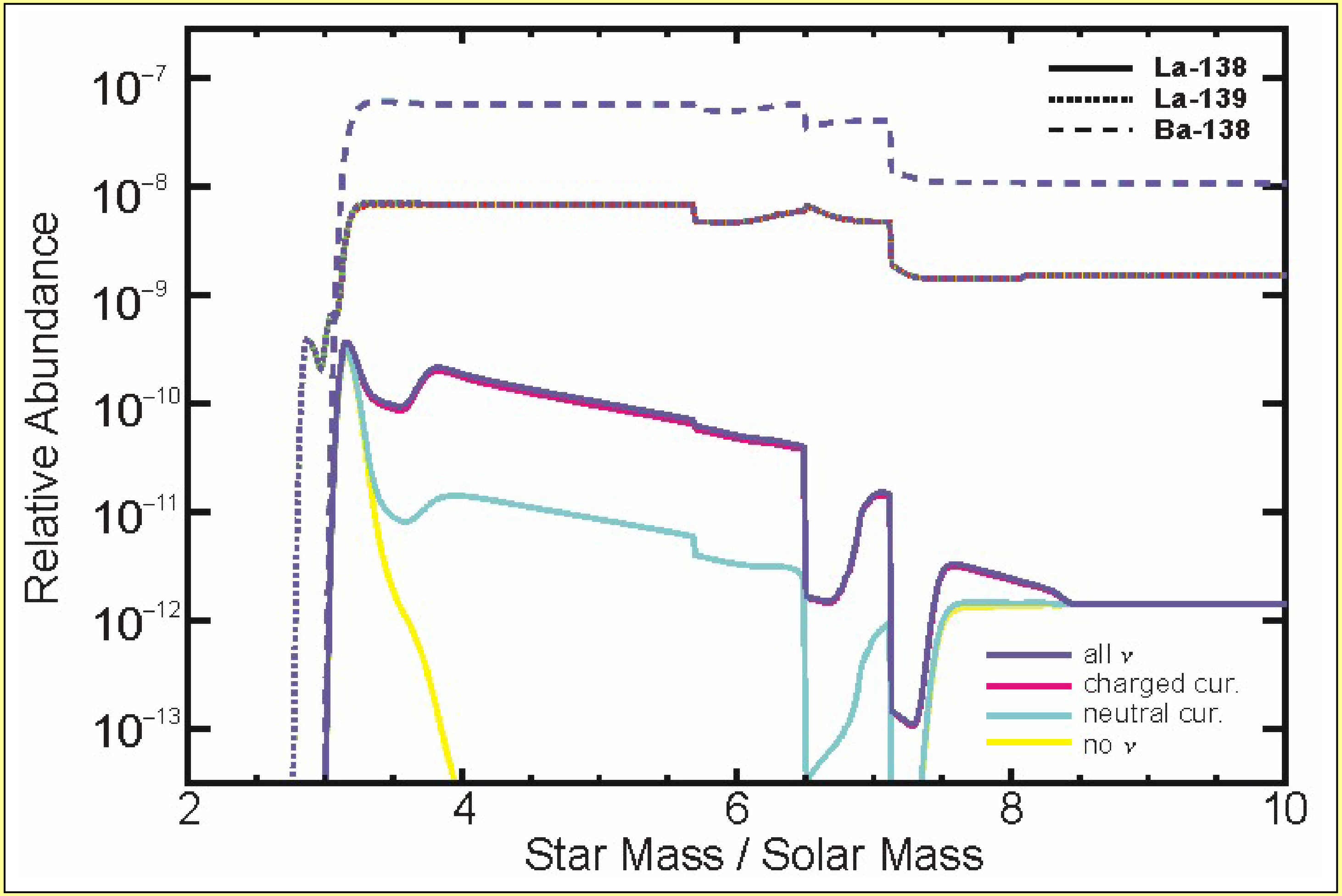

- ^{138}La: pure ν process production
- ^{180}Ta: 50% ν process, 50% *p* process

Theoretical prediction

- Low neutrino energies → small q → $\Delta L = 0$ → GT strength

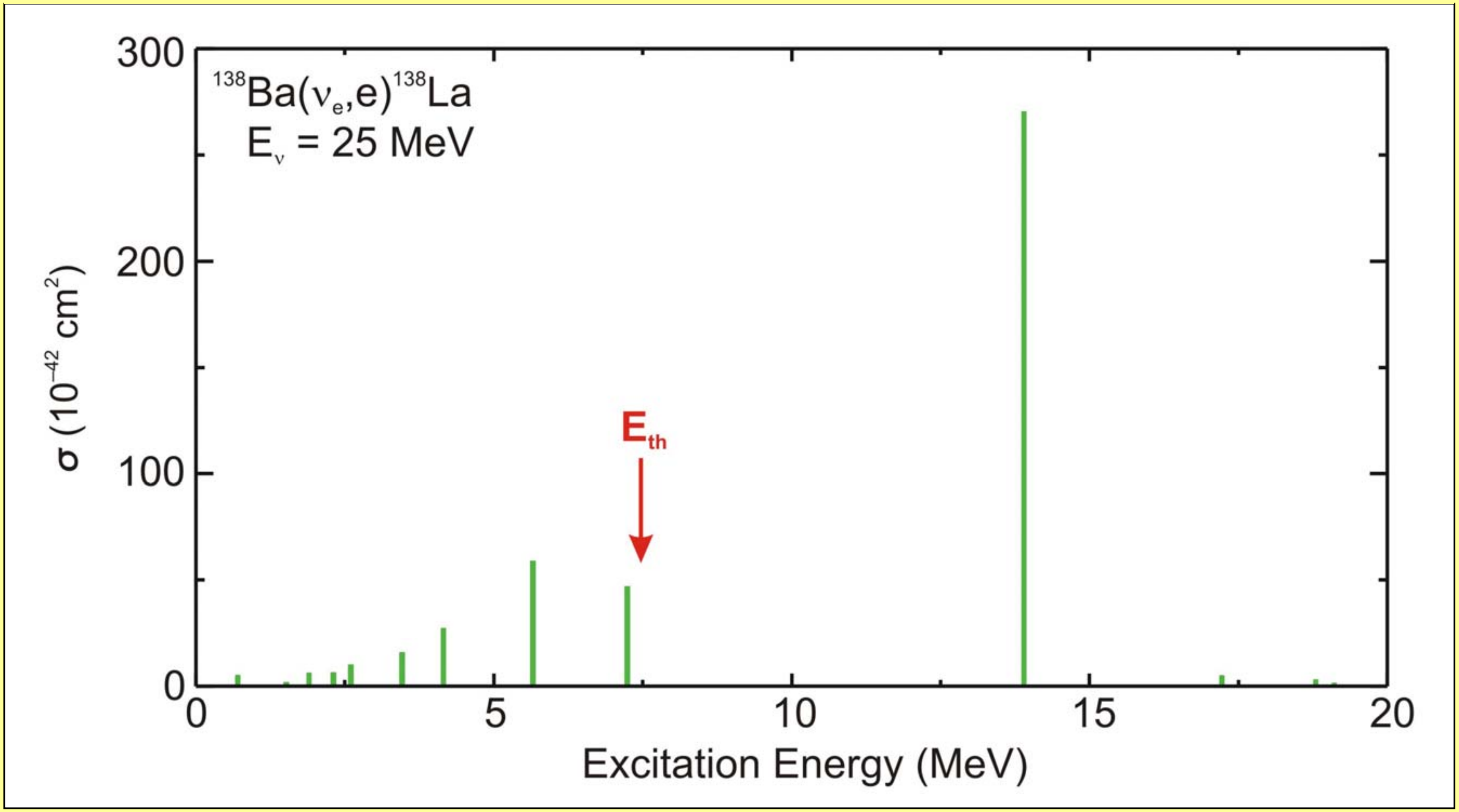

- RPA predicts main GT resonance well above neutron threshold
- Predictions for the low-lying strength are questionable

Experimental requirements

- (ν_e,e) → Gamow-Teller strength ← (*p*,*n*) or (^{3}He,*t*)
- Gamow-Teller part → narrow angle cut around 0°
- Intermediate energies → simple one-step reaction mechanism

Grand Raiden

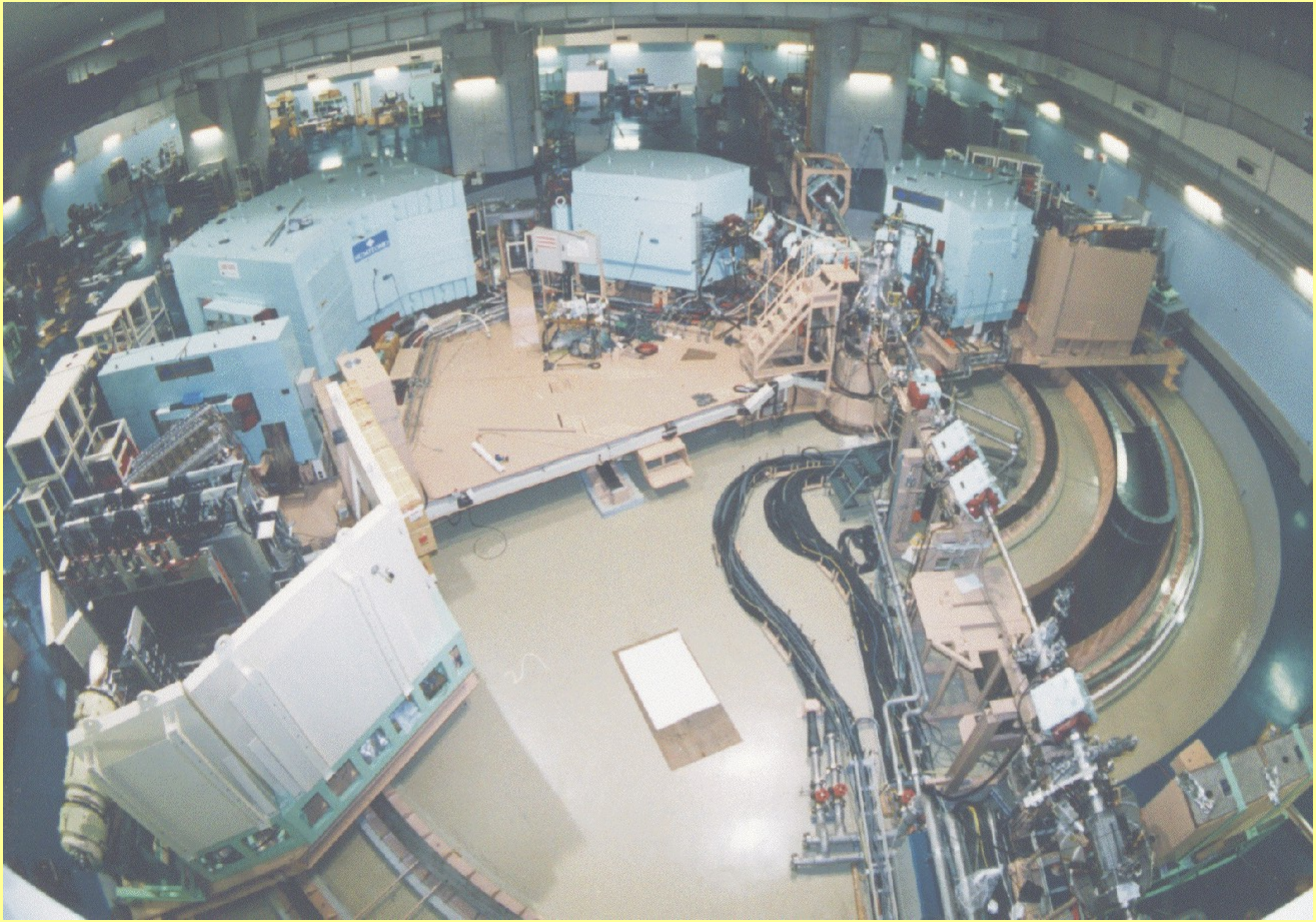

^{138}La spectrum

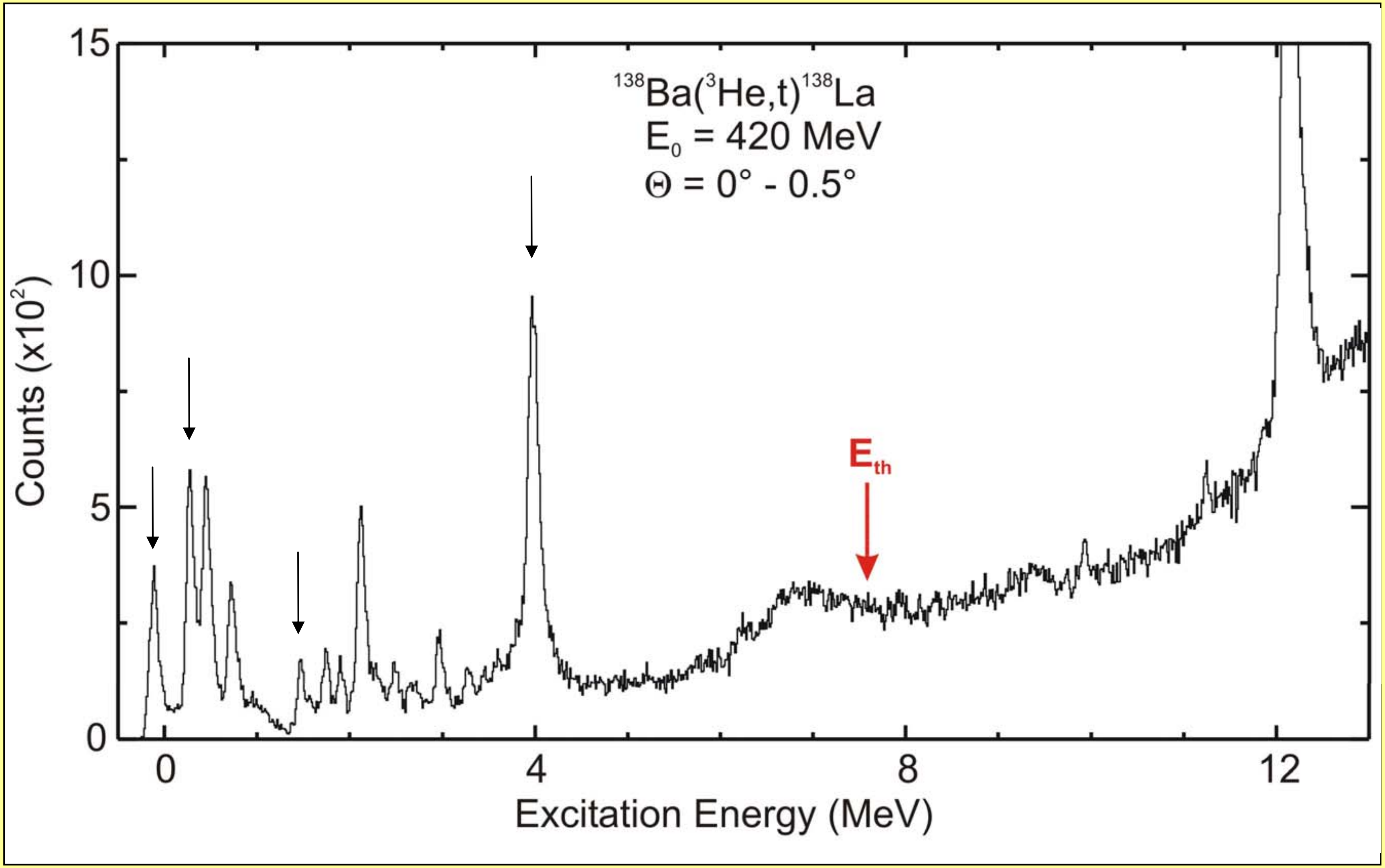

- Target: $^{138}BaCO_4$ embedded in polyvinylalcohol (PVA)

GT strength distribution in ^{138}La

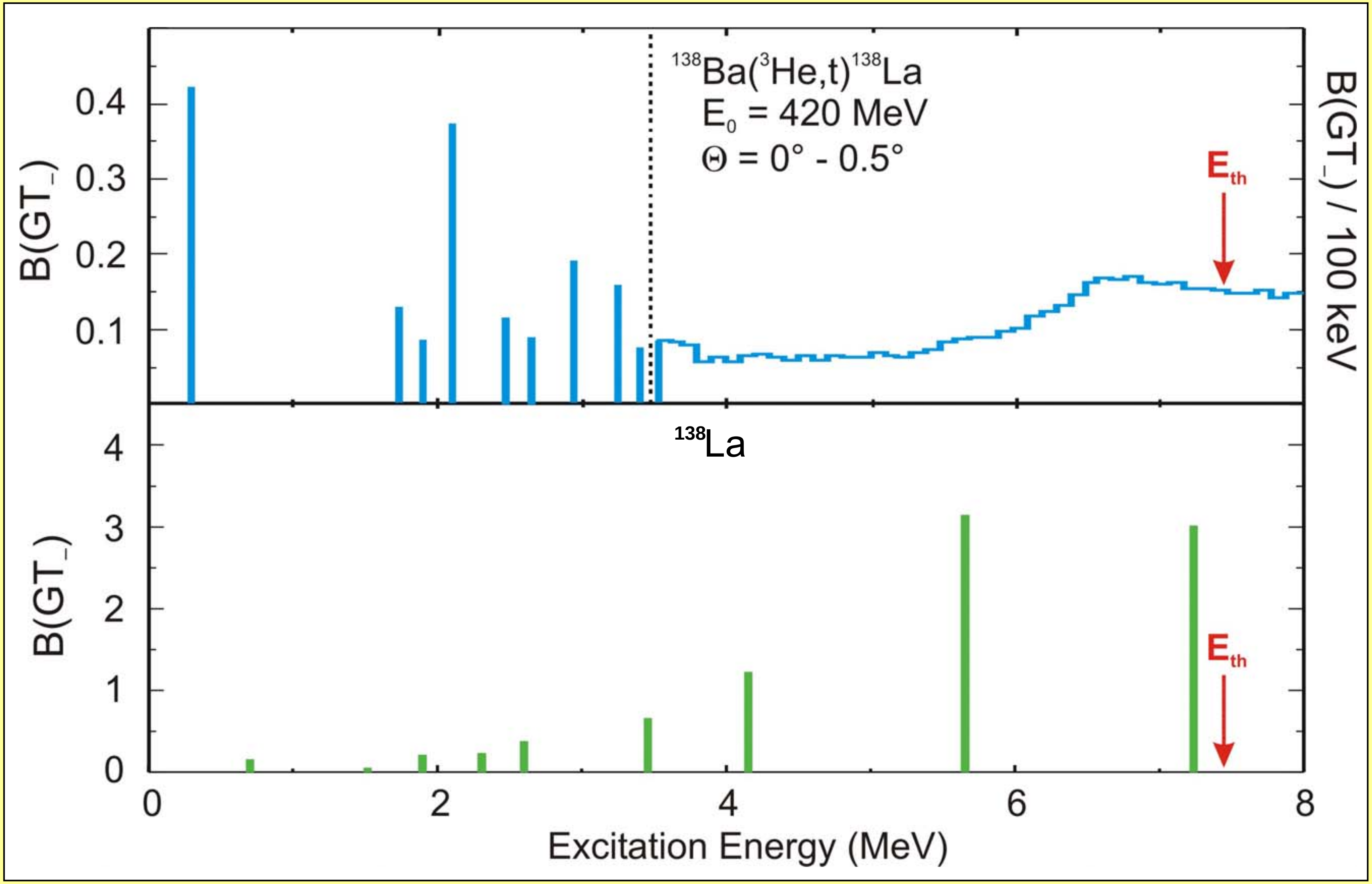

Cumulated strength for ^{138}La

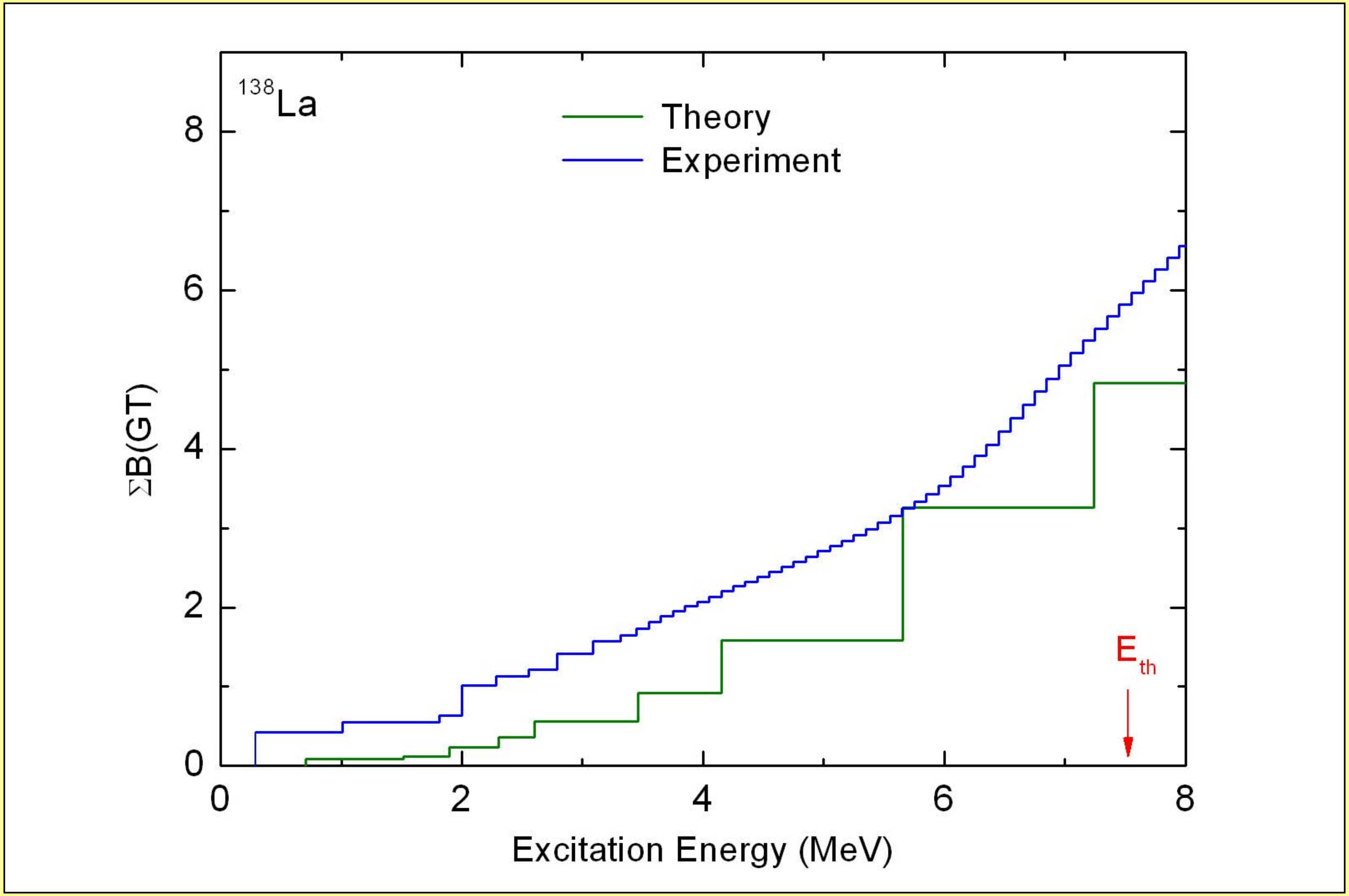

- $B(GT_{-})_{exp} \approx 1.17 \cdot B(GT_{-})_{theo}$ at 7.47 MeV

Cumulated strength for ^{180}Ta

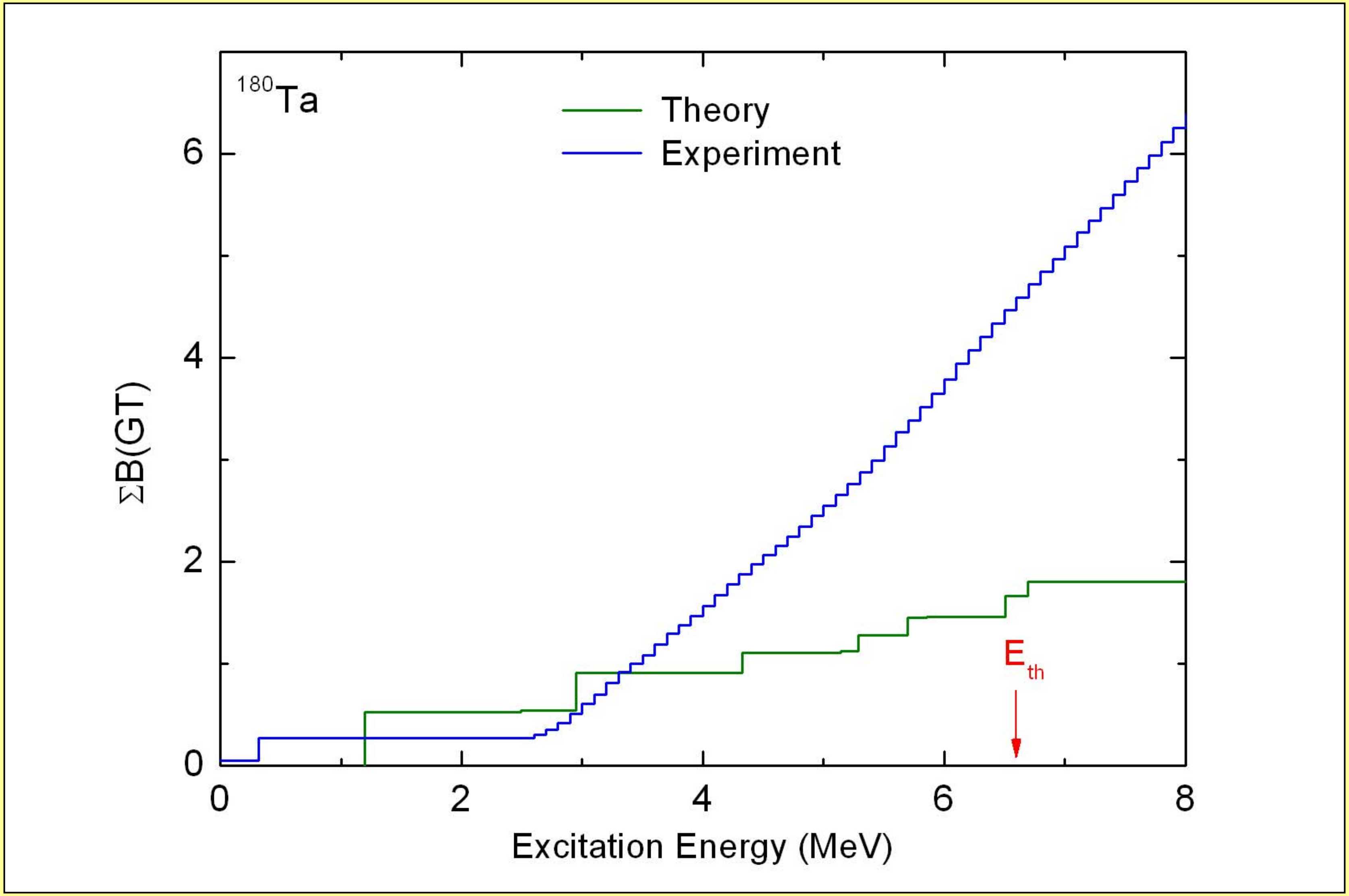

- $B(GT_-)_{exp} \approx 2.76 \cdot B(GT_-)_{theo}$ at 6.64 MeV

Yields of ^{138}La and ^{180}Ta for a 15 $M_\odot$ star

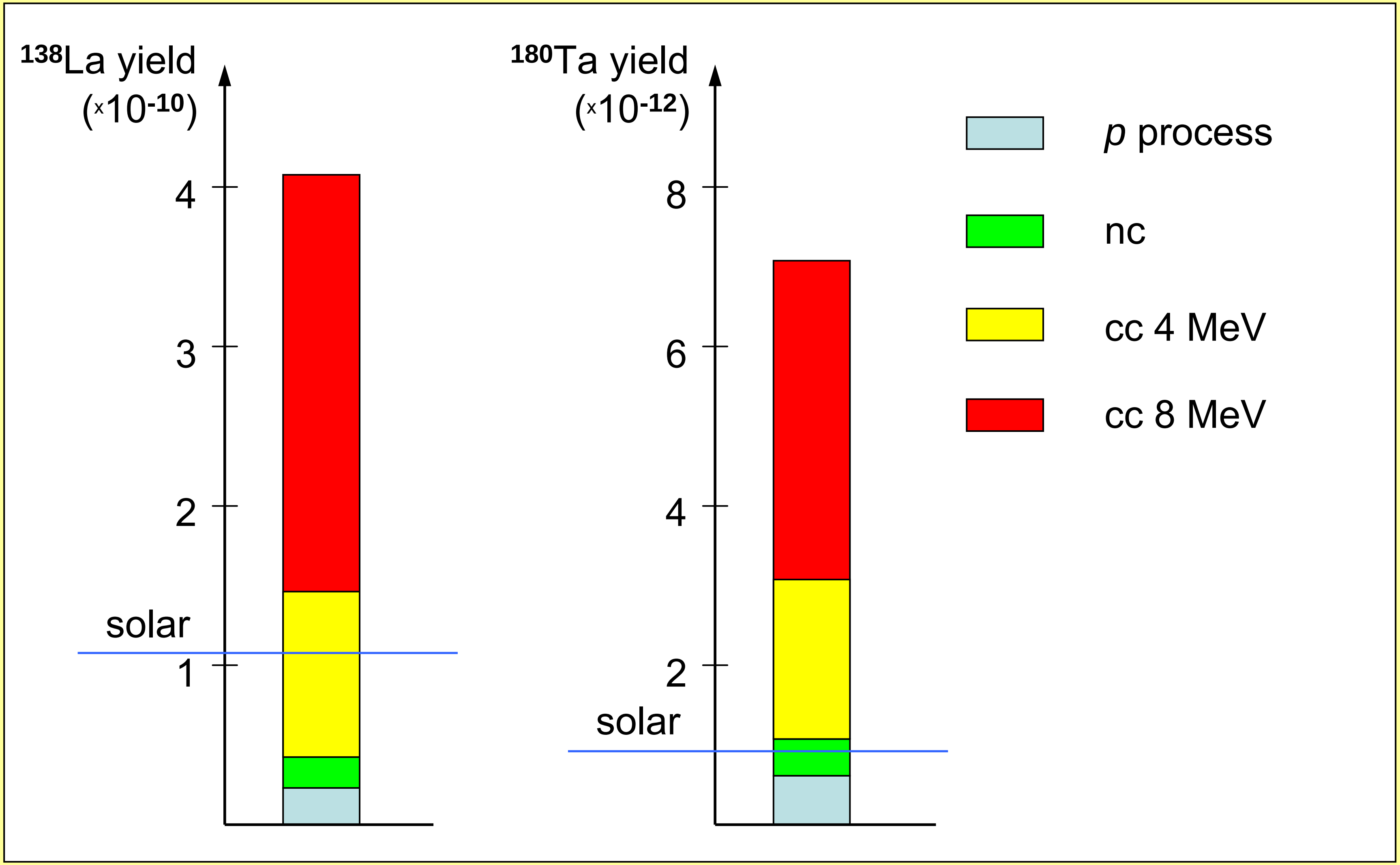

- Solar abundances are reproduced by neutral and charge current reactions
- Branching ratio to ^{180}Ta isomer neglected

Conclusions

- GT strength in ^{138}La and ^{180}Ta below particle threshold extracted
- ^{138}La is essentially produced in the ν process
- ^{180}Ta at least partially produced in the ν process

Collaborations

- $^{2}H(e,e')$

  TU Darmstadt / U of Mainz / U of Saskatchewan / Washington U

- $^{9}Be(e,e')$

  Chalmers TU / TU Darmstadt

- $^{12}C(e,e')$

  TU Darmstadt / GSI Darmstadt / MSU

- $^{52}Cr(e,e')$

  TU Darmstadt / GSI Darmstadt

- $^{138}Ba(^{3}He,t)^{138}La$
  $^{180}Hf(^{3}He,t)^{180}Ta$

  U of California / TU Darmstadt / GSI Darmstadt / iThemba LABS /
  Los Alamos / RCNP and Osaka U